ARTIFICIAL INTELLIGENCE APPLICATION IN COVID-19 DIAGNOSIS AND PREDICTION USING BY CT SCAN

A THESIS SUBMITTED TO THE INSTITUTE OF GRADUATE STUDIES OF NEAR EAST UNIVERSITY

BY

ÖZCAN UZUN

IN PARTIAL FULFILLMENT OF THE REQUIREMENTS FOR THE DEGREE OF MASTER OF SCIENCE

IN

ELECTRICAL ELECTRONIC ENGINEERING

NICOSIA, T.R.N.C – 2021

Approval

We hereby certify that the thesis title "ARTIFICIAL INTELLIGENCE APPLICATION IN COVID-19 DIAGNOSIS AND PREDICTION USING BY CT SCAN" has been defended by ÖZCAN UZUN on the 4th October, 2021 and accepted in partial fulfilment of the requirement for the degree of Master of Science in Electrical Electronic Engineering.

Thesis committee

Name signature

Chair of committee and supervisor: Assoc. Prof. Dr Sertan SERTE
Near East University

Member: Assist. Prof. Dr Ali SERENER
Near East University

Member: Assist. Prof. Dr Elbrus Bashir İMANOV
Near East University

Approved by: Prof. Dr. K. Hüsnü Can BAŞER
Director Institute of Graduate Studies
Near East University

……

I hereby declare that all information in this document has been obtained and presented in accordance with academic rules and ethical conduct. I also declare that, as required by these rules and conduct, I have fully cited and referenced all material and results that are not original of this work.

Name, Last name:

Signature:

Date:

ACKNOWLEDGEMENTS

I readily take this opportunity to express profound gratitude to my supervisor Assoc. Prof.Dr. Sertan Serte for his supervision, correction during the term of my candidature. Without his valuable contribution and assistance, this piece of work would not have been completed.

I also extend gratitude to the dean Prof.DrBülent Bilgehan to all the lecturers and professors of the department of electrical and electronic engineering, staff and course mate, in Near East University; Prof. DrŞenol İbrahim Bektaş,Prof. DrTerin Adalı,Prof. DrNadire Çavuş,Assoc. Prof. Dr Boran Şekeroğlu, Assoc. Prof. Dr Dilber Uzun Özşahin,Assoc. Prof. Dr Yöney Kırsal Ever,Asst. Prof.DrKaan Uyar,Assoc. Prof. Dr. Fezile Özdamlı, Asst. Prof. DrSahar Ebadinezhad for their constructive suggestion and correction which was made without expectation.

Sincere recognition goes to the Uzun family and also to my friends Valerie Oru Agbor, Ali Şanlı, Haldun Özcan, Fatih Birol, Erhan Derviş Kara just to name a few for their moral and financial support, as well as their sacrifices throughout this research work.

I am eternally grateful to God Almighty for providing me with the mental and physical capabilities, as well as the chance to do this work.

ABSTRACT

When we look at the present world we can see easily that humanity is fighting a deadly catastrophe Covid-19 which the World Health Organization(WHO) declared a pandemic. The main element that constitutes Covid-19 is Coronaviruses. They are a large group of viruses that cantrigger sickness in living organisms including humans. Some of these viruses are known to cause respiratory diseases. These viruses range from flu to more extreme illnesses. The disease has caused havoc on the economy and society, risking the lives of tens of millions of people and increasing the number of individuals who are malnourished.Diagnosing this disease due to its inconveniences to individuals, families, and states is very important, PCR is widely used as a diagnostic procedure of covid-19, medical imaging which we considered CT-scan is also good due to its ability to show lungs images. Since pneumonia is one of the symptoms found in a majority of patients suffering from covid-19, a chest CT scan has proven to be an effective screening and diagnosis. The application of artificial intelligence to evaluate COVID-19 CT scan images diagnosis and prediction during this global pandemic of COVID-19 has also shown great improvements. Within the scope of this study, we used CNN models such as AlexNet and VGG 16. Especially to get exact results, Deep learning models Alex Net and VGG were used here to show an accuracy of 67% and 75%, the sensitivity of 72% and 86%, specificity of 64% and 70% respectively.

Keywords:**Artificial intelligence,COVID-19, machine learning, deep learning, x-ray/CT Scan,CNN, AlexNet,VGGNet.**

ÖZET

Günümüz dünyasına baktığımızda, insanlığın son iki yıldır Dünya Sağlık Örgütü tarafından pandemi olarak ilan edilen Covid-19 olan ölümcül bir felaketle tüm dünyada mücadele ettiğini rahatlıkla görebiliriz. Covid-19'u oluşturan ana unsur Coronavirüslerdir. Coronavirüsler, insanlar da dahil olmak üzere canlı organizmalarda hastalığa neden olabilen geniş bir enfeksiyon grubudur. Bu virüslerin bazılarının solunum yolu hastalıklarına neden olduğu bilinmektedir. Bu virüsler gripten daha aşırı hastalıklara kadar çeşitlilik gösterir. Salgın ekonomiye ve topluma zarar verdi, on milyonlarca insanı aşırı yoksullukla tehdit etti ve etkilenen insan sayısını artırdı. Kişilere, ailelere ve devletlere verdiği sıkıntılar nedeniyle bu hastalığın teşhis edilmesi çok önemlidir, teşhiste PCR yöntemi covid-19 için tanısal bir prosedür olarak yaygın olarak kullanılmaktadır, CT taraması olarak değerlendirdiğimiz tıbbi görüntüleme sistemleri akciğer görüntülerini gösterebilmesi nedeniyle daha avantajlıdır. COVID-19 hastalarının genelinde pnomoni tespit edildiği için, göğüs bilgisayarlı tomografi (BT) taramasının teşhis ve tanıda net , hızlı çözümler üretildiği gösterilmiştir. Bu küresel COVID-19 salgını sırasında COVID-19 CT tarama görüntülerinin teşhisini ve tahminini değerlendirmek için yapay zekanın uygulamaları da büyük gelişmeler göstermiştir. Bu çalışma kapsamında Derin öğrenme yöntemleri ve bunların alt modelleri olan Evrişimli Sinir ağları (CNN) kullanılmıştır. Özellikle kesin sonuçlar elde etmek için, burada sırasıyla %67 ve %75 doğruluk, %72 ve %86 duyarlılık, %64 ve %70 özgüllük göstermek için Derin öğrenme modelleri Alex Net ve VGG kullanılmıştır.

AnahtarKelimeler: **Yapay zeka, COVID-19 Teşhisi, Makina öğrenimi, Derin öğrenme, Röntgen ,Bilgisayarlı tomografi,Evrişimli sinir ağları,AlexNet,VGGNet**

TABLE OF CONTENT

LIST OF TABLES

LIST OF FIGURES

LIST OF ABBREVIATIONS

BiLSTM: Bidirectional Long Short-Term Memory

CT: Computed Tomography

CNN: Convolutional Neural Network

DL: Deep Learning

DNN: Deep Neural Network

DRAW: Deep Recurrent Attention Writer

GRU: Gated Recurrent Units

GUPs: Graphical Processing Units

IR: Image retrieval

LTMS: Long Short-Term Memory

MERS-CoV: Middle East Respiratory Syndrome

RBNA: Radiological Society of North America

RT-PCR; Real-Time Polymerase Chain Reaction

RNN: Recurrent Neural Network

DL: Deep Learning

SARS-CoV-2: Serious Acute Respiratory Syndrome

VAE: Variational AutoEncoder

VGG: Visual Geometry Group

WHO: World Health Oeganization

CHAPTER 1: INTRODUCTION

1.1 Introduction

Coronavirus disease is an infectious illness that can be transmitted from person to person, also object to persons it is known for causing severe acute respiratory syndrome. On the 12 of the third month of the year 2020, World Health Organization (WHO), declared the sickness a pandemic after it swiftly spread throughout the globe (WHO, 2020). The illness that caused the 2019 new coronavirus epidemic is given an official designation by the World Health Organization. December 2019, saw the emergence of a new coronavirus, now known as SARS-CoV-2, trigger severe respiratory illnesses in Wuhan, a city in the Hubei Province of China. On February 11, 2020, COVID-19 became officially the name of the sickness caused by this virus. Coronavirus Disease 2019, or COVID-19, is the new name for this illness. Corona, VI, and D, are the abbreviations for Corona, Virus, and Disease. The disease was previously known as the "2019 novel coronavirus," or "2019-nCoV."The virus is spreadable from person to person and has caused a worldwide epidemic. The mortality rate continues to rise, forcing many governments to impose social separation and lockout policies. The absence of adequate treatment or cure is a big problem. According to epidemiological data, elderly people are more susceptible to acute illnesses, whilst children have milder symptoms (Yuki et al., 2020). Coronavirus disease 2019 (COVID-19) is a form of coronavirus pneumonia that causes severe acute respiratory illness (SARS-CoV-2). SARS-CoV-2 infection generates clusters of severe respiratory illness, similar to the coronavirus that causes SARS. Human-to-human transmission has been observed via droplets, contaminated hands, and surfaces with incubation durations ranging from 2 to 14 days. Early diagnosis, seclusion, and supportive therapy are required to treat patients (Zhai et al., 2020). Artificial intelligence (AI) was first acknowledged as a distinct science in the mid-twentieth century, followed by cycles of optimism and disappointment as the discipline progressed to its current prominence, where various aspects of AI touch practically every aspect of modern technology. Much of the sector's success in recent decades has been ascribed to advances in computer power, enormous digital databases, and, as a result, the emergence of cloud computing infrastructures, as well as a greater grasp of theoretical AI features and implementable algorithms. Technological leaders including IBM, Google, Microsoft, Apple, and Facebook were actively developing AI by the first decade of the twenty-first century. Speech may now be used to instruct technical gadgets on how to do jobs. In medical, the program can identify

individual people inside photographs by detecting specific pathological abnormalities in computed tomography (CT) or other images of the physical body, or specific ill characteristics in computed tomography (CT) or other images of the physical body. The main goal is to create hardware and software that allows a computer to perform cognitively challenging activities like decision making. AI is a broad field that includes a number of subfields, each of which approaches the problem in a different way. Algorithms are trained to do certain tasks in machine learning by learning patterns from big datasets. DL is a sort of ML where massive volumes of data are merged with artificial neural networks inspired by human brain planning to solve extremely complicated issues. (Chartrand et al., 2017; Erickson et al., 2017).

1.2 Applications

Early detection of infected persons is a key step in controlling COVID-19. Using radiography and radiology images to detect the disease is one of the quickest techniques to diagnose patients. Several investigations found distinct abnormalities in COVID-19-infected individuals' chest radiographs. We investigate the use of Artificial Intelligent models to identify people suffering from covid and chest radiography pictures, based on previous studies (Asif et al., 2020). A chest CT scan can help diagnose, detect complications, and forecast the outcome in people who have a Coronavirus infection (COVID-19). The clinical value of chest CT in this disease will be increased by taking proper preventative safety precautions, optimizing chest CT technique, and establishing a structured reporting system based on pulmonary results. Chest CT scans, contrary to popular assumption, can give both false-negative and false-positive results. Furthermore, a variety of complex factors, the most important of which is resource availability, influence the added value of chest CT in diagnostic decision-making (RT-PCR tests) (Kwee & Kwee, 2020). Identifying this condition is essential due to the challenges it causes people, families, and states. This takes us to another diagnostic technique in medical imaging, the CTscan. Because pneumonia is present in the majority of COVID-19 patients, thoracic computed tomography (CT) scans may be useful for screening and diagnosis. Furthermore, CT has the benefit of producing results swiftly (Bernheim A. et al,2020). A chest CT scan can reveal ground-glass regions with or without reticulation (so-called "crazy paving pattern"), consolidative pulmonary opacities in late stages, and therefore the "reverse halo" sign (Huang C. et al. 2020). In the early stages of COVID-19, CT scanning has an advantage over chest X-rays because peripheral patches of ground glass are a symptom of

early COVID-19 and can be easily missed on chest X-rays (Rubin GD. et al, 2020). Some studies show that CT scanning might assist distinguish between positive and negative COVID-19 (Li Y. & Xia L., 2020). CT's value, on the other hand, is contested due to a rumor lack of discriminating utility. This argument is further complicated by the fact that PCR sensitivity may be poor, making it impossible to compare the two tests (Xie X. et al, 2020). In addition, the value of a diagnostic test can be impeded by illness frequency, and evidence on CT performance in a population with a modest COVID-19 prevalence is sparse. This method/technique also allows for the use of additional technologies, like AI, and it does more, not just in terms of diagnostics, but prediction as well. COVID-19's effect on lung tissue is considered to be monitored via chest X-ray imaging (Radiology Assistant, 2020). As a consequence, COVID-19 may be detected using chest X-ray pictures.

CHAPTER 2: LITERATURE REVIEW

2.1 Introduction

As the number of cases climbs, most countries are running out of testing kits and equipment. We built a Deep Learning model to assist radiologists and doctors in recognizing COVID-19 patients using chest X-rays because to the limited number of testing kits available and the rising number of regular cases (Khan et al., 2020). The method of specimen collection sometimes really makes people uncomfortable. And to solve this problem means all infected persons ought to be identified and treated but most importantly the method of detection or diagnostics hence how fast and accurate the diagnostic technique. With all that is been said AI applications could be just what is required. Since 1979, scientists have made significant advances in deep neural networks, which emerged as a distinct branch in 2006, in an unsupervised approach, machine learning research was used to reduce the dimensionality of data. When it comfortably defeated the runner-up in the ImageNet competition in 2012, it caught the attention of academics. The visual information from a huge number of photographs was automatically extracted and classified using a deep convolutional neural network (CNN). Active deep learning research has been conducted to handle complicated problems in practically all fields of study since then. Picture identification, speech recognition, semantic picture segmentation, lingual processing, and a variety of other tasks have all obtained cutting-edge results (Ahmad J. et al., 2019). Deep learning refers to a group of machine learning techniques aimed at automatically extracting key features from data write Hinton et al (2012). DNNs are artificial neurons with input, hidden, and output layers, similar to standard neural networks. Deep networks, on the other hand, have a lot of hidden layers, unlike ordinary neural networks. Deep neural networks may uncover properties at numerous levels, each of which corresponds to a distinct amount of generalization, thanks to their hierarchical construction. According to Le Cun et al. (2015), basic characteristics are learned in the early levels and then presented in the profound layers to construct relatively high concepts. It is frequently used to spread data such as pictures, music, and text. Significantly improved multiprocessing capabilities of hardware, particularly general-purpose graphics processing units (GPUs), dramatically increased data size available for training, and thus recent advances in machine learning techniques are the most important reasons for deep learning's acceptance. Deep learning techniques may now readily apply

complicated, compositional nonlinear functions, automatically learn distributed and hierarchical features, and employ both labeled and unlabeled data(Ahmad J. et al., 2019).

2.2 Deep learning for covid-19 classification using x-ray images

COVID-19 is a novel virus that targets the upper and lower respiratory systems. The number of infections and deaths has steadily escalated to the point that a global pandemic has emerged. Lung X-ray images were recently found to be beneficial in tracking the COVID-19 illness, which may be used to track a variety of lung disorders. To distinguish COVID-19 and normal (healthy) chest X-ray images, deep learning-based approaches such as deep feature extraction, fine-tuning of pretrained CNN, and end-to-end training of an existing CNN model were used. Deep CNN models (ResNet18, ResNet50, ResNet101, and so on) were used to extract deep features. To extract deep characteristics, deep CNN models were used (ResNet18, ResNet50, ResNet101, VGG16, and VGG19). The fine-tuning technique also uses the previously mentioned pretrained deep CNN models (Ismael & Sengür, 2021).Figure 2.1: Illustration of deep learning methods for COVID-19 Detection.

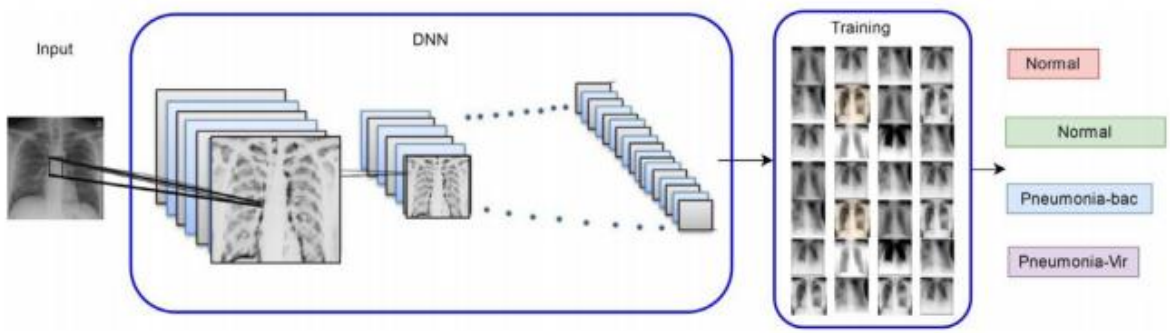

Figure 2.1: Illustration of deep learning methods for COVID-19 Detection (Ismael &Şengür, 2021)

2.3 Deep learning for covid-19 classification using CT scan images

With the use of computed tomography (CT) scan pictures, COVID-19 screening can be done rapidly and accurately. The recommended technique's deep learning process is based on a CNN. CTnet-10 models, for example, may accurately diagnose COVID-19 by using various deep learning algorithms to differentiate between COVID-19 and non-COVID-19 CT scan images. DenseNet-169, VGG-16, ResNet-50, InceptionV3, and VGG-19 are among the other models used. Of all the classifiers examined, the VGG-19 was the most accurate. Doctors can employ COVID-19 automated diagnostics with CT scan images as a

quick and effective technique to diagnose COV. Doctors can employ COVID-19 automated diagnosis with CT scan images as a quick and effective COVID-19 screening tool (Shah et al., 2021). See figure 2.2.

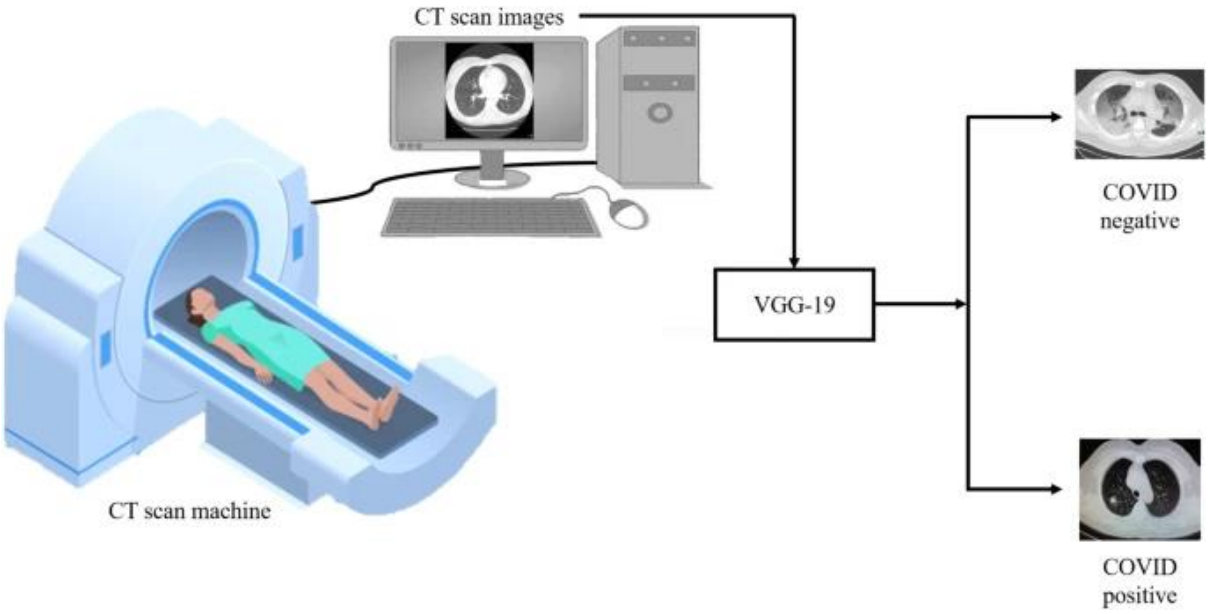

Figure 2.2: A graphical representation of a CNN model in the classification of COVID 19 using CT scan images (Shah et al., 2021)

A schematic depicts the system's movement. A CT scan image of a patient is generated by the CT scan equipment for COVID-19 screening. A VGG-19 model is used to identify whether the input image is positive or negative in terms of COVID-19.

2.4 Datasets for x-ray scans

2.4.1 NIH Chest x-ray dataset images

The National Institutes of Health (NIH) published the Chest x-ray dataset X. Wang et al, (2017), which contains 108,948 pictures of 32,717 unique individuals grouped into 8 distinct categories, some of which may overlap. The radiologists' annotations were labeled using natural language processing techniques (see figure 2.3).

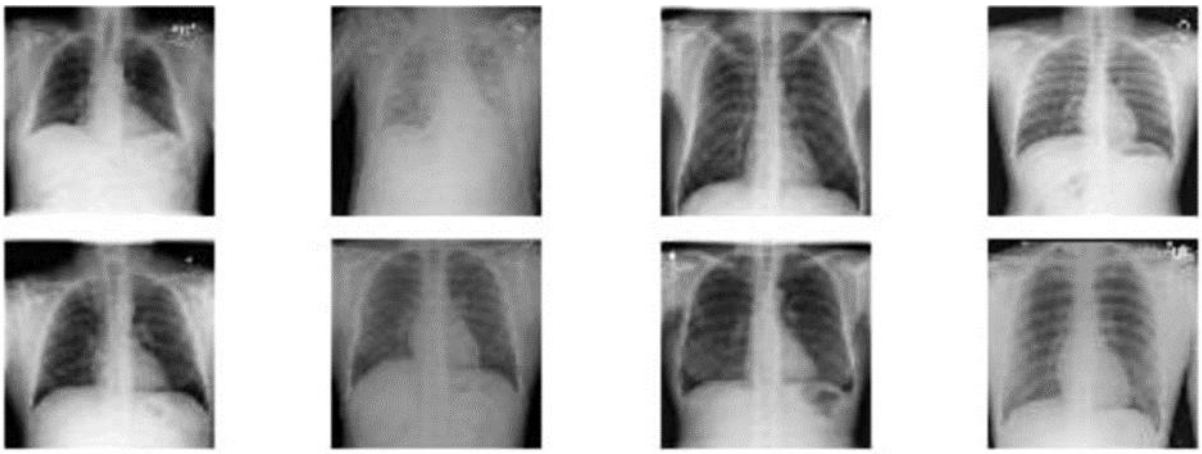

Figure 2.3: Samples from the NIH dataset (Maguolo & Nanni, 2021)

2.4.2 Chexpert (CHE) Chest x-ray dataset images

Chexpert, a huge dataset of more than two hundred thousand chest radiographs from more than 60 thousand patients divided into 14 groups, was collected and labeled by Irvin et al. (2019). The natural language processing-based tagging strategy used in this new dataset surpasses the one used in Chestx-ray8 (CHE). See figure 2.4

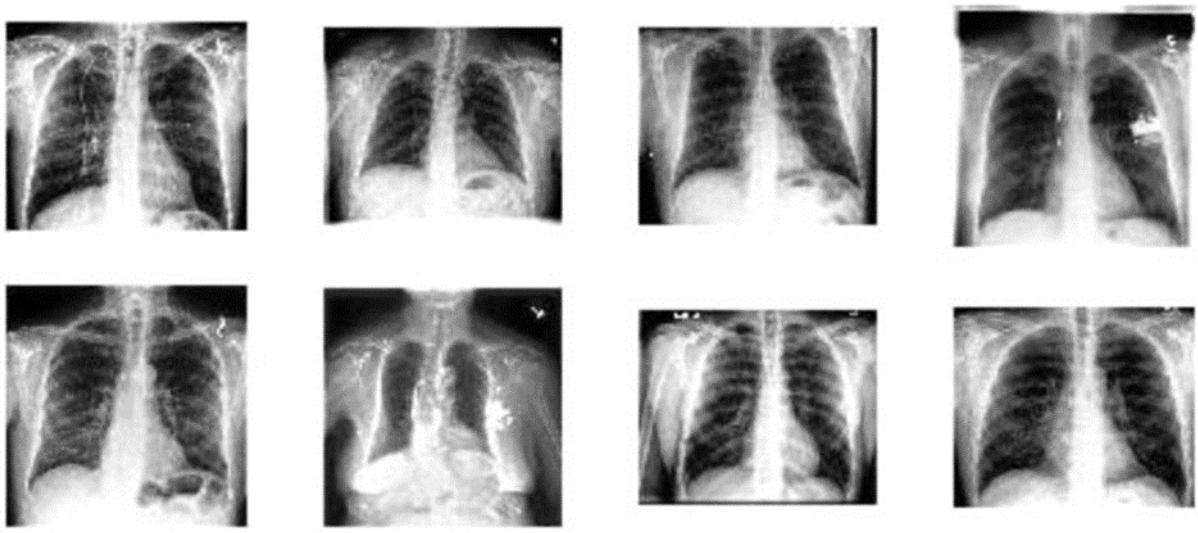

Figure2.4: Samples from the CHE dataset (Maguolo & Nanni, 2021)

2.4.3 Kaggle (KAG) Chest x-ray dataset images

Dr. Paul Mooney devised a Kaggle competition in 2017 to divide viral and bacterial pneumonia into categories(https://www.kaggle.com/paultimothymooney/chest-xray-pneumonia/version/2). It varies from the previous datasets in that it includes 5863 pediatric photographs. This dataset is known as KAG, see figure 2.5 with a few examples.

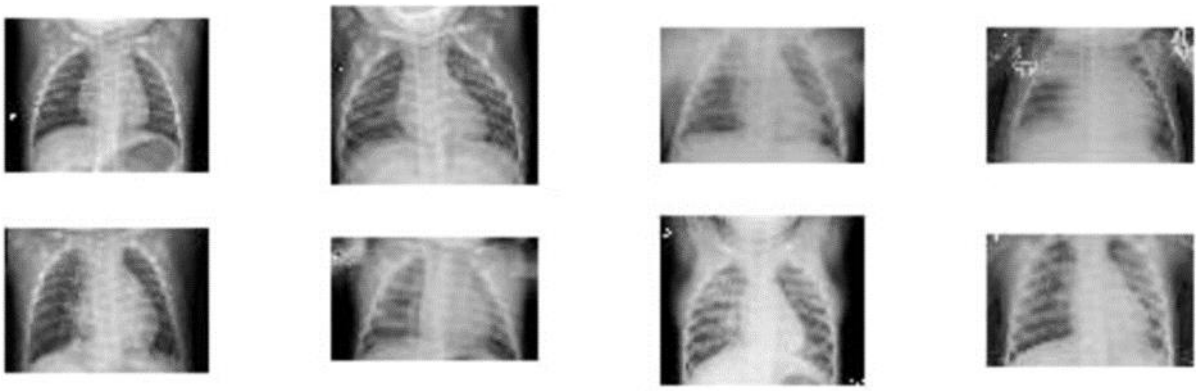

Figure2.5: Samples from the KAG dataset, (www.kaggle.com/paultimothymooney/chest-xray-pneumonia/version/2)

2.4.4 Dataset images for covid 19 chest x-ray

COVID-19 photos come from the repository made available by Cohen et al. (2020), which is the main source of most COVID-19 research. The database presently has 144 images of frontal x-ray scans of people who may have COVID-19. Every sample contains information such as the patient ID and, in most cases, the location, as well as additional remarks such as a reference to the doctor who took the images. Figure 2.6 illustrates a selection of the samples.

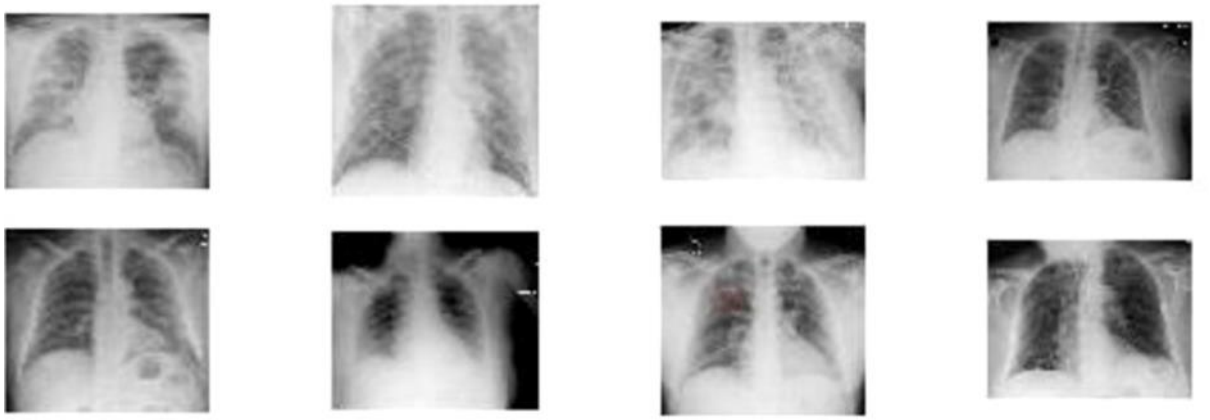

Figure2.6: Samples from the COV dataset, (www.kaggle.com/tawsifurrahman/covid19-radiography-database)

Deep learning is based on data, which is utilized to feed these models of learning. Because COVID-19 is a new disease, there are no relevant datasets for this investigation. As a result, in order to construct a dataset, we required to obtain chest X-ray images from two different publicly available image databases. Joseph et al. have made COVID-19 X-ray pictures available in an open-access GitHub repository (2020). For research purposes, the

writers collected radiological photographs of COVID-19 cases from a range of authorized sources and the bulk of COVID-19 studies employ photos from this source. At the registration, there is an open database. The repository maintains an open collection of COVID-19 chest X-ray or CT images, which is regularly updated. At the time of publication, the database contained around 290 COVID-19 chest radiography images. Photos of bacterial, infected, and regular chest X-rays were available in the Kaggle repository "Chest X-Ray Images (Pneumonia)" (2020). The dataset contains 1203 natural Pneumonia, 660 bacterial and 931 viral Pneumonia cases. From these two sources, we gathered 1300 photos. The photos were then downsized to 224 224 pixels in size and 72 dpi resolution. See figure 2.7.

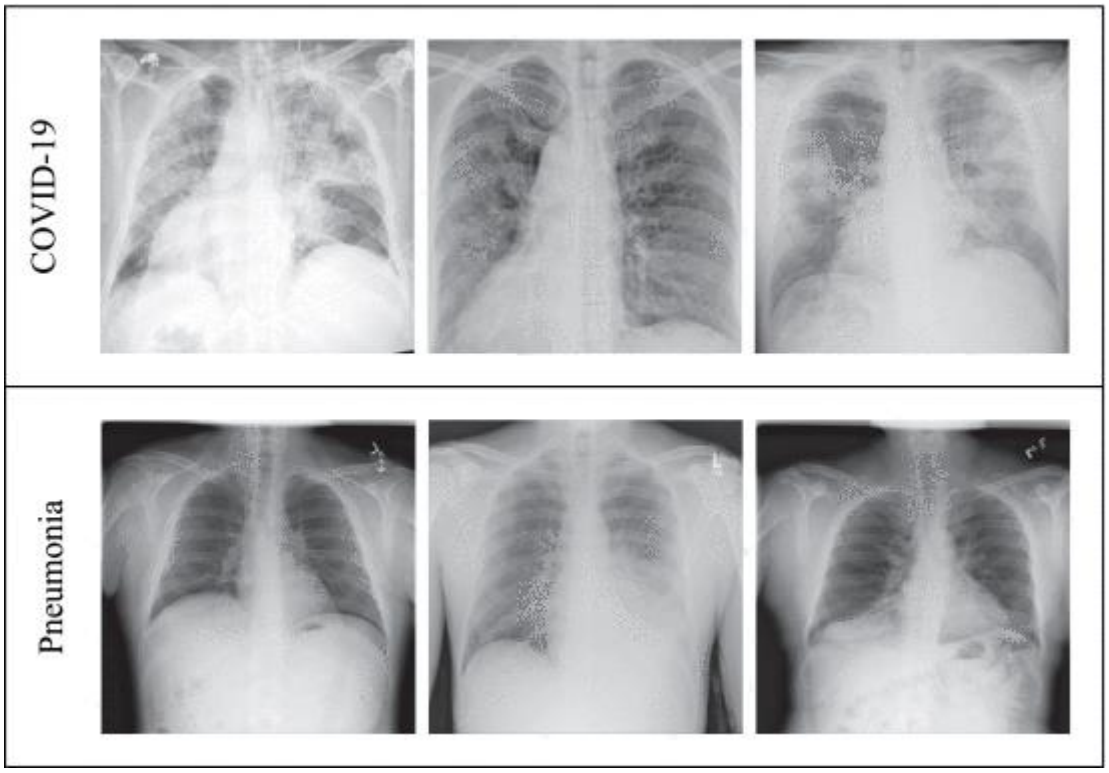

Figure 2.7: Sample X-Ray images of COVID-19 and Pneumonia from a prepared dataset (GitHub repository 2020).

2.4.5 X-Ray dataset table

The main characteristics of the various datasets are listed in Table 2.1.

Table 2.1. Summary of the 4 Datasets.

Dataset	COV	NIH	CHE	KAG

Covid Samples	144	0	0	0
Healthy Samples	0	84,312	16,627	1583

Natural Discourse Processing (NLP) is an algorithm-based method for decoding and manipulating human language. This approach is one of the most extensively used fields of machine learning. This specialization will teach you how to use cutting-edge deep learning techniques to create cutting-edge NLP systems. See table 2.2.

Table 2.2. Dataset summary.

Disease	Normal	Pneumonia Bacterial	Pneumonia Viral	COVID-19
No. of Images	310	330	327	28

2.5 Datasets for CT scans

2.5.1 Datasets for CT images

During the COVID-19 epidemic, CT is a valuable technique in diagnosing its patients. Because of privacy concerns, publicly available COVID-19 CT datasets are extremely difficult to get, hampered research and development of AI (deep learning)-powered diagnostic techniques for COVID-19 assisted CTs. See figure 2.8.

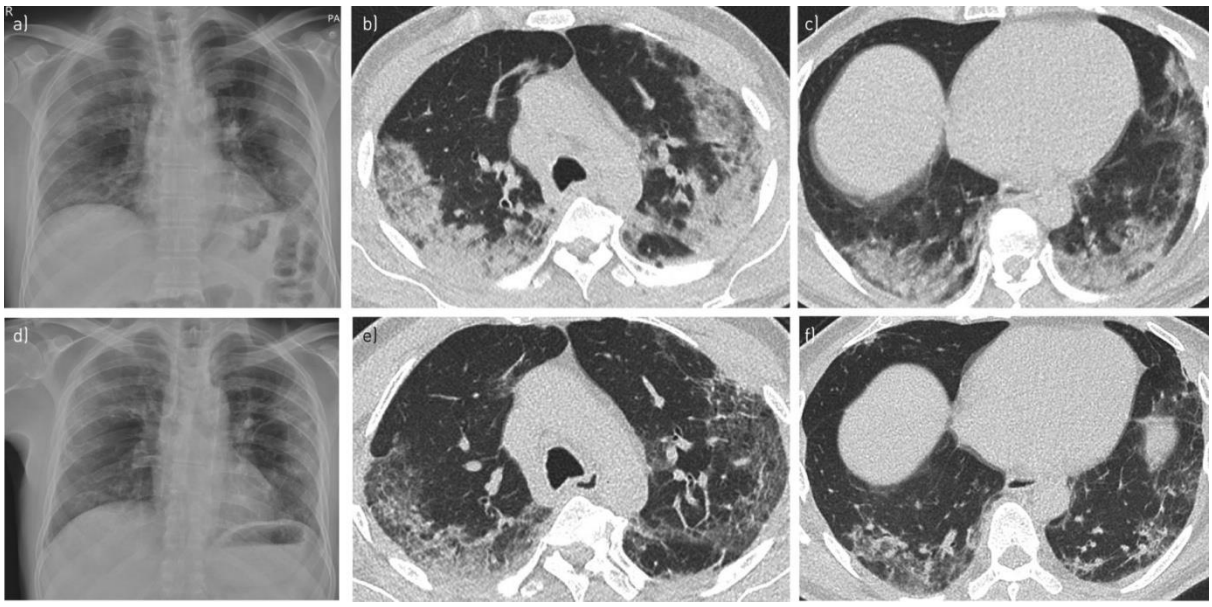

Figure 2.8: sample CT scan images (Jacob, J. et al., 2020).

The pictures of a 61-year-old man who arrived with a seven-day history of nausea and shortness of breath are shown in Figure 2.8. a) A chest radiograph revealed patchy peripheral consolidation in the middle and lower zones at the time of admission. Axial CT

images of the b) upper and c) lower lung zones on day 6 of hospitalization indicated multifocal peripheral consolidation, which was compatible with the diagnosis of COVID-19. d) A 3.5-week chest radiograph showed considerable consolidation clearance, which was confirmed by repeat CT imaging of the e) upper and f) lower lung zones, albeit with some architectural deformation inside the lungs. Artificial intelligence approaches can help assess disease progression trends in COVID-19 when applied at scale to imaging and related clinical data. Unsupervised deep learning algorithms could aid in the identification of different COVID-19 patient features associated with different illness trajectories. Image analysis may also help forecast which patients are more likely to have chronic multisystem sequelae after an acute illness, which could affect future healthcare resource allocation (Jacob, J. et al., 2020).

2.5.2 CT Scan Dataset table

NA is an acronym that stands for "not available." Datasets from computed tomography scan COVID-CT-MD and COVID-19 for machine learning and deep learning. This table gives CT scan dataset from different sources and different label types, as shown on table 2.3.

Table 2.3. COVID-19 CT scan datasets that are currently accessible.

Covid-19	CAP	Normal	Label type	Data source	References
49	NA	NA	Significant	Multiple	Bjorke, H. (2020)
20	NA	NA	Significant	Multiple	Jun M. et al., (2020)
20	NA	NA	Significant	Multiple	Cohen J. et al., (2020)
856	NA	254	Classification	Multiple	Morozov S. et al. (2020)
216	NA	55	Classification	Multiple	Zhao J. et al., (2020)
60	NA	60	Classification	Multiple	Soares E. et al., (2020)
95	NA	282	Classification	Single	Rahimzadeh M. et al., (2020)
2980	NA	NA	Classification	Multiple	Jacob, J. et al. (2020)
169	60	76	Classification	Single	COVID-CT-MD

The COVID-19 CT scan dataset, designated COVID-CT-MD, can be used in COVID-19 categorization machine learning and deep learning experiments. The COVID-CT-MD dataset contains 169 confirmed positive COVID-19 cases (collected from 2020/02/23 to 2020/04/21) as well as 76 normal patients (collected from 2019/01/21 to 2020/05/29) and 60 Community Acquired Pneumonia (CAP) cases (collected from 2018/04/03 to 2019/11/24). All of these examples were acquired from the Babak Imaging Center in Tehran, Iran, and labeled at the patient, slice, and lobe levels by three trained radiologists. The "patient-level label" refers to the individual's diagnosis, whereas "slice-level" and "lobe-level" pertain to detecting infected slices and lobes, respectively. In addition, all participants get full access to the CT volume. COVID-CT-MD is shown in Table 2.3.

CT scans are created by stitching together cross-sectional 2D images of thin body sections (slices) to create a 3D representation of the body's components. A spinning X-ray generator fires a stream of X-ray photons at the item from various angles in current CT scanners. Sensitive radiation detectors collect the amount of radiation that passes through the item, and using image reconstruction methods, a computer-assisted methodology reconstructs the information from the detectors into detailed sequential images. Dhawan, A. P. (2011). The helical acquisition approach, which involves moving the patient along the gantry while the X-ray beams and detectors circle swiftly around them, was used to capture all COVID-CT-MD pictures in axial view with a SIEMENS SOMATOM Scope scanner. Filtered Back Projection (FBP) is used to rebuild the pictures (Katsevich, A. 2002).

2.6 Machine Learning Algorithms

New opportunities arose as a result of the rapid growth of science and technology. Several sorts of theoretical knowledge, such as statistics and complicated algorithms, are incorporated into automated devices that are powered by technology. A simple study of machine-learning algorithms can serve as a starting point for future machine-learning development. This will enhance the use of machine-learning algorithms, which will aid the sector's economic growth.

2.6.1 Supervised Learning

Controlled learning is a simple learning strategy used in the machine learning process. This technique of learning entails defining each person's particular learning goals prior to learning. It is dependent on information technology to comprehend the need for learning

during the machine's initial training. We will gradually finish the necessary study material in a controlled environment in order to acquire essential knowledge. In comparison to other learning strategies, supervised learning may activate the machine's generalized learning capabilities. After finishing system learning, it can assist people in solving some classification or regression problems in a very systematic manner. Traditional learning methods such as BN, SVN, KNN, and others are currently in use. Because the entire learning process has a purpose, the entire learning process is regular, and the learning material is more methodical as a result (Li K. & Jiang S., 2020).

2.6.2 Unsupervised Learning

Uncontrolled learning is the other way around. Uncontrolled learning means that throughout the learning process the machine does not mark the material in any particular direction, but trusts the machine to complete the knowledge information analysis. In practice, the operating approach is used to enable a machine to acquire the essential ideas and content, then to allow the machine to accomplish series of content learning encompassing concepts and materials nearly as fundamental as tree roots. The fragmented growth of learning has generally extended the spectrum of machinery. Uncontrolled learning includes techniques like autoencoders and deep-belief networks. This is conducive to clustering issues solving and has practical implications for the development of a variety of companies (Jiang Na et al.,2019).

2.6.3 Reinforcement Learning

Besides supervised and unsupervised learning, machine learning consolidation apprenticeship approaches also exist. Systematic learning is referred to as strengthening learning in a specific subject. The information gathered throughout the previous time will be used during the specific application procedure. It organizes and analyzes feedback input from a specific area to create a closed knowledge processing loop. In general, improving learning is a type of learning strategy that uses statistics and dynamic learning to improve data collection. These methods are mostly used to address the problem of robot control (Cuocolo et al., 2020). The Q-learning algorithm is two of the most renowned learning algorithms of its kind.

2.7 Deep learning

In deep neural networks, which emerged in 2006 as a unique area of engine learning research when used to decrease the size of data in an unattached manner, scientists have

since 1979 achieved tremendous strides. It won the ImageNet competition by a huge margin in 2012, attracting the attention of researchers and defeating them. Deep convolutional neural networks (CNNs) were utilized to extract visual features and categorize a large number of photos automatically. To solve complicated problems, deep learning research has been conducted in practically all subject domains. The best results were achieved in image identification, voice recognition, semantic pictures, language processing, and a variety of other tasks (Yasaka et al., 2018). According to Hinton and colleagues in 2012, DL is a category of ML algorithms seeking to automatically uncover the fundamental properties of data. Deep neural networks (DNN), like standard neural networks, include artificial neurons organized into input, hidden, and output layers. However, unlike traditional neural networks, deep networks generally include a large number of hidden layers. Deep neural networks' hierarchical structure enables them to discover characteristics at several levels, each of which corresponds to a different degree of abstraction (Tirumala & Narayanan, 2015). Basic characteristics are learned in the first tiers and then presented in the deeper layers to build higher-level ideas. It is frequently used for a variety of data types such as pictures, audio, and text. For deep learning to be successful, hardware multiprocessing capabilities, notably general-purpose graphics processing units (GPUs), vastly improved data availability, and current advances in machine learning algorithms must be used. By using non-linear functions successfully, deep learning algorithms may now automatically learn distributed and hierarchical characteristics, as well as work with both, labelled as well as unlabeled data (Ahmad et al., 2018). It's possible to split the methods into three categories: deep networks for unsupervised or supervised and hybrid techniques. We'll take a quick look at each of these techniques in a moment.

Deep networks for supervised learning: these networks can recognise and predict patterns. The network attempts to differentiate between data components of different classes depending on the labels supplied, however, it is not always effective. The network learns to link input to anticipated output in classification and regression tasks, helping it to generate more accurate predictions (label). DNN, CNN, and recurrent neural networks are examples of supervised learning architectures (RNN). To form a hierarchy, each layer of a DNN uses a different type of neuron. The preceding layer's output is then used as an input for the next. From the input files, each subsequent layer learns additional patterns. Higher layers

are in charge of learning high-level knowledge, whereas lower layers are in charge of learning low-level information (Ahmad et al., 2019).

2.7.1 Classification of Deep learning methods

Deep learning methods are classified into three types: unsupervised deep networks, supervised deep networks, and hybrid approaches. We'll go through these techniques briefly presently.

2.7.1.1 Deep networks for supervised learning:

Deep neural networks for supervised learning: deep neural networks can recognize and predict patterns. The network tries to discriminate between data components of different classes depending on the labels provided, however it is not always effective. In classification and regression tasks, the network learns to link input to expected output, allowing it to make better predictions (label). DNN, CNN, and recurrent neural networks are examples of supervised learning architectures (RNN). Every DNN layer uses a variety of neurons to build a hierarchy. The preceding layer's output is then used as an input for the next. Each succeeding layer learns more input file patterns. Lower layers pick up low-level information, whereas higher layers pick up high-level data (Ahmad J. et al., 2019).

Because of its multiple layer structure, Deep Neural Network is the most basic of this type. See figure 2.9.

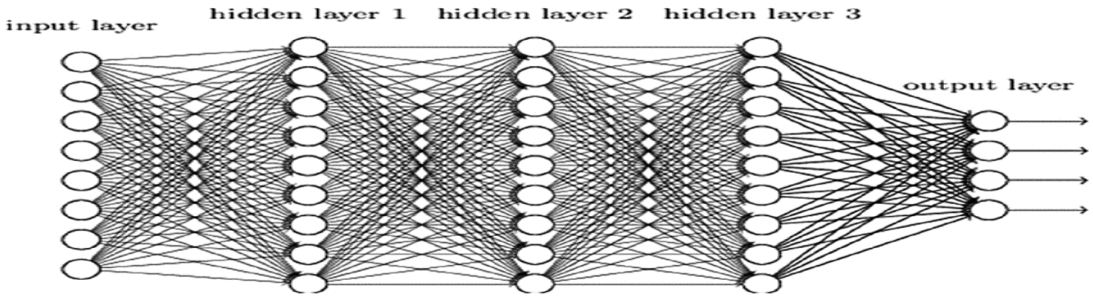

Figure 2.9: A fully connected feed-forward deep neural network, (Valentin Radu, 2018)

CNN, which was created in 1979, is another well-known supervised learning architecture that was created specifically for visual processing such as photographs and movies. They've also been proven to work with nearly any type of data, including visual, audio, and text. The three types of layers are convolutional, pooling, and fully connected CNNs. To learn fundamental qualities that will appear in the data, the convolution layers use filters/kernels whose coefficients are adjusted throughout the training period. To construct

a feature map, each filter is convolved independently over the input, with higher activation values indicating the location of features. The CNN's lowest layers, like DNNs, learn simple features, while the kernels learn more and more advanced properties as we progress deeper into the network. The pooling layers, according to Ahmad et al. (2017), reduce the complexity of feature maps while also creating a point of translation invariance inside the network. The network's features extraction process is formed of the convolutional and pooling layers, which identify local characteristics within the input. The local features are then combined by the fully linked layers to provide global features. Despite being established earlier, it wasn't until thirty-three years later, in 2012, that CNNs gained prominence when they won the renowned ImageNet competition by an outsized margin. Alex Net was a convolutional neural network of five layers, three pooling layers, and three fully connected layers, see figure2.10

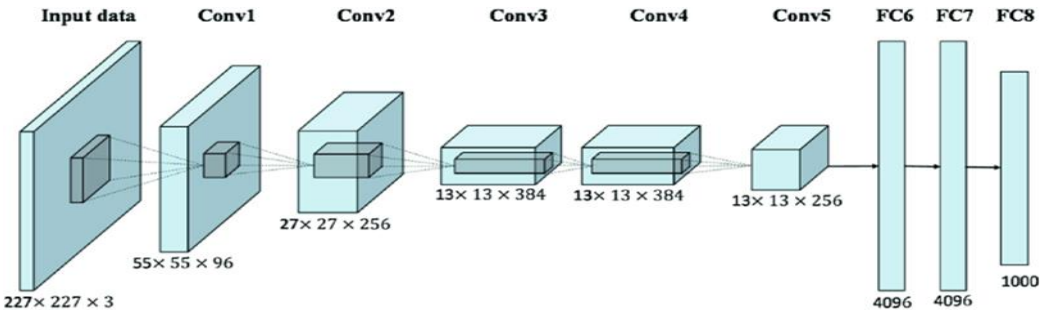

Figure 2.10: Convolutional neural network architecture (AlexNet)(Han et al., 2017)

Recurrent Neural Network (RNN) is a supervised learning deep network that was built to find patterns in time series data that DNN and CNN could not, despite their strength. Each RNN unit includes recurrent connections, which allows the network to store data for longer periods of time. This enables the RNN to recognize patterns in sequential data such as audio, film, and text. Long STM (LSTM) networks are a newer and more advanced type of RNN that boosts the capacity of RNNs for pattern recognition. (Ullah et al. 2018). See figure 2.11

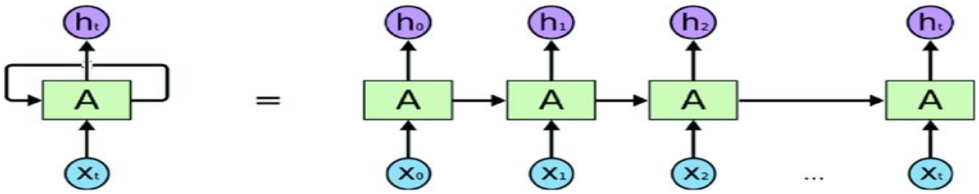

Figure 2.11: Architecture of a single recurrent unit in Recurrent Neural Network (RNN)(https://denizyuret.github.io/Knet.jl)

2.7.1.2 Deep networks for unsupervised learning

Throughout the learning process, unsupervised learning refers to learning systems that do not give task-specific supervision information (such as target class labels). Deep autoencoders and deep Boltzmann machines are two of the most widely used approaches for unsupervised learning (DBM). Autoencoders and deep bottleneck networks have two components. The main component tries to keep the input file size as small as possible. The second component reconstructs the initial input from this truncated representation. The autoencoder tries to build a compact representation that can be used to recover the original data with the least amount of loss during training. This method employs unsupervised learning of extremely significant aspects of the training data. The compact representation of the autoencoder is widely employed as a feature vector of the high-dimensional input for tasks like as clustering, indexing, and searching, as well as dimensionality reduction and feature embedding (Hinton & Salakhutdinov, 2006). See figure 2.12

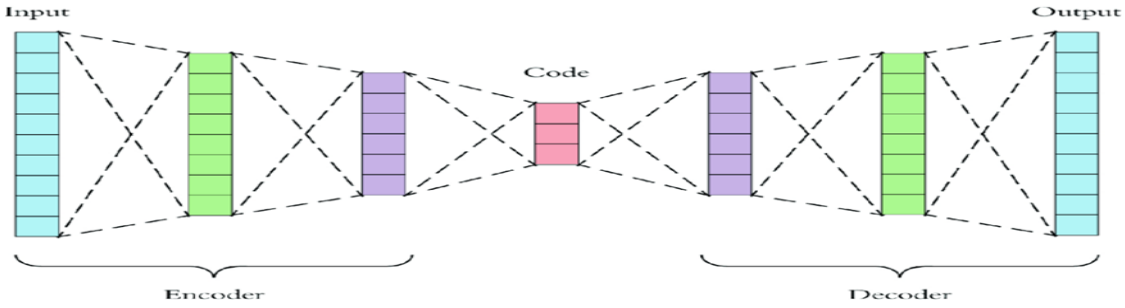

Figure 2.12: Architecture of a simple autoencoder demonstrating the encoder and decoder parts (Charte et al., 2020)

DBMs (deep Boltzmann machines) are probabilistic generative models made up of several random layers. The top two layers are connected by symmetric, undirected connections, whereas the lower levels are connected by directed connections from the layer above them from the top down (Lu et al. 2017).

2.7.1.3 Hybrid approach

Discrimination could be the goal of the third category, which is often supported by the findings of a generative or unsupervised deep network. It's commonly done in supervised learning to improve deep network optimization and regularization. For example, in the unsupervised learning technique, a huge amount of unlabeled data could be used to generate the starting parameters for the subsequent supervised learning job. The method

can be used to estimate parameters in any unsupervised deep network using unsupervised learning when supervised learning discriminative criteria are not available.

2.7.2 Applications of Deep Learning

In many applications, profound knowledge has been employed, including computer vision, voice identification, virus detection, x-rays and cars amongst others. The availability of vast amounts of data, combined with extremely competent algorithms, has created enormous potential for academics to develop cutting-edge technologies. The analysis of multimedia content to solve difficult problems is highly competency-rich in deep learning algorithms including CNNs, RNNs, and LSTMs. The CNNs are ideal for classifying images, objects and objects, segmenting, increasing and restored images and video frames. RNNs and LSTMs, on the other hand, are used in applications such as video event detection, speech recognition, and text image recognition to process sequential data. The two designs can also be used in conjunction to resolve complicated problems. CNNs, for instance, are employed as function extractors while LSTMs are utilized to discover patterns for event/action recognition in video frames (Qin et al., 2019). Both might alternatively be trained independently on the desired task before being combined during the inference phase. Furthermore, there is a great improvement of these approaches in past years, and we anticipate further advancements in the future. Below are just a few of the breakthroughs; computer vision, information retrieval, Natural Language Processing and multi-task learning. The following are just a few of the breakthroughs;

2.7.2.1 Computer vision

Advances in deep learning have aided a variety of industries, including computer vision. It has allowed computers to do human-level image identification, object recognition, and image segmentation.

2.7.2.2 Information retrieval

IR make it possible for people to acquire important information quickly and easily. Images, music, and text can all be used to represent data. Machine learning and deep learning, in any event, are critical to achieving IR's goal.

2.7.2.3 Natural language processing

This is a subfield of Artificial Intelligence and Linguistics that teaches computers how to make human language assertions or words. Natural processing of the language was designed to facilitate the life of the user and to satisfy his need to interact in the natural

language with the computer. As not all users have a good knowledge of a particular language on their machines, NLP offers those who do not have sufficient time to study or perfect new languages. A language can be either a set of rules or a set of symbols. Symbols are combined and used to transmit or broadcast data; it is also used in nuclear medicine (oncology). The Rules maintain a totalitarian grip on symbols. Natural Language Processing is split into two parts: Natural Language Understanding and Natural Language Generation, both of which include the process of comprehending and producing text (Collobert & Weston 2008).

2.7.2.4 Multitask learning

To accomplish our goal in machine learning, we usually train one or more models (ML). We'll also try fine-tuning model settings and changing models until they reach the desired performance or stop growing. Although focusing on a single task often results in satisfactory performance, the information we neglect could help us perform even better on the metric that matters to us. This type of information is mostly acquired from training signals gathered from other operations.

2.7.3 Deep learning methods in covid 19 diagnostics

Accurate short-term forecasting of new infected and recovered patients is critical for maximizing existing resources and preventing or delaying the spread of such diseases. Deep learning models have recently made significant progress in managing time-series data in a range of applications. There are about five deep learning methods for forecasting the number of new cases and recovered cases. COVID-19 occurrences were forecasted globally using the Simple Recurrent Neural Network (RNN), Long short-term memory (LSTM), Bidirectional LSTM (BiLSTM), Gated recurrent units (GRUs), and Variational AutoEncoder (VAE) approaches (Zeroual et al., 2020).

2.7.3.1 Recurrent neural networks

In a variety of applications, regular feedforward neural networks have proven to be effective. In such networks, data flow transformations are communicated in one way through hidden layers, with the output entirely influenced by the current circumstance. However, because these neural networks have limited memory, they are inappropriate for modeling historical data sequencing and temporal correlations. Recurrent neural networks (RNNs) for time-dependent learning challenges have been created to solve these issues. RNNs are based on the notion of taking prior data into consideration while generating

output. To do this, cells representing gates that change the output based on past observations are added to the output. RNNs are depicted schematically in Figure 13. A segment of a neural network, A, evaluates some input xt and generates a value ht. RNNs are very good at learning temporal information (I. Oksuz et al., 2019).

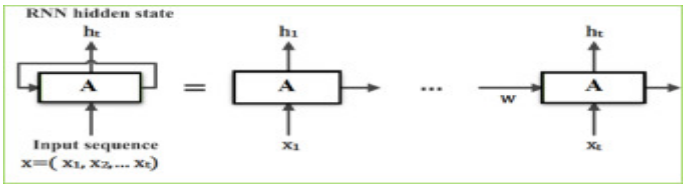

Figure2.13. Schematic presentation of RNN (colah.github.io/posts/2015-08-UnderstandingLSTMs)

LSTM and GRU are two efficient RNN models for time-dependent data in time-series data. In a variety of applications, traditional networks have proven to be capable of providing good time series results.A. Ashour et al., F. Harrou et al., F. Harrou et al., F. Harrou et al., F. Harrou et (2020). When compared to traditional time series models, these deep learning models have demonstrated to be more effective at modeling and forecasting. The LSTM and GRU models' essential architecture is depicted in the diagrams below. See figure 2.14

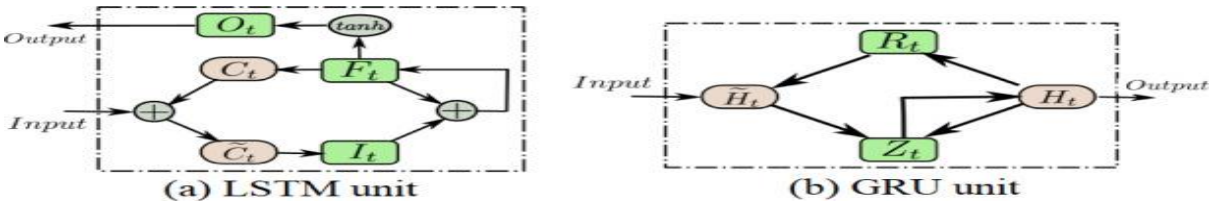

Figure2.14: Basic structures of LSTM unit and GRU unit (K. Cho et al.,2014)

The basic structure of the LSTM and GRU models is shown in Figure 14. (a) In the LSTM, the letters It, Ft, and Ot represent input, forget, and output gates, as well as C and memory cell capacity. (b) Reset and update gates are present in Rt and Zt, respectively, but candidate hidden state and hidden state are present in Htand and Htand, respectively.

2.7.3.2 LSTM models

The LSTM, created by S. Hochreiter and J. Schmidhuber in 1997, is a complicated gated memory device designed to circumvent the fading gradient affects that limit RNN output. The gradient becomes either too tiny or too large in the event of the important time stage,

resulting in a vanishing gradient issue. During training, the optimizer backpropagates and forces the process to execute even when the weights rarely move. The three gates that regulate the flow of information in an LSTM are the input, forge, and output gates. These gates are mostly made up of logistic functions of weighted sums, the weights of which are determined during training using backpropagation. The input gate and forget gate are used to keep track of the status of the cell. The output gate, also known as the hidden state, generates an output that represents the memory in use. This procedure allows the network to remember for an extended period, which is not feasible with a single RNNS. The improved ability of LSTM to recognize long-term dependencies and manage time-series data are both desired properties.

2.7.3.3 Bidirectional LSTM

The current state of the LSTM may only be reconstructed using the backward sense, as previously indicated. The LSTM model, on the other hand, disregards the forward meaning because it is linked to the current state. The BiLSTM approach was created by combining the favorable qualities of the bidirectional RNN M. Schuster & K. Paliwal (1997) with those of the LSTM A. Graves & J. Schmidhuber (2005) to overcome this restriction and improve its rebuilding accuracy. This was accomplished by merging two hidden states that allow data from both the backward and forward layers to flow freely. See figure 2.15

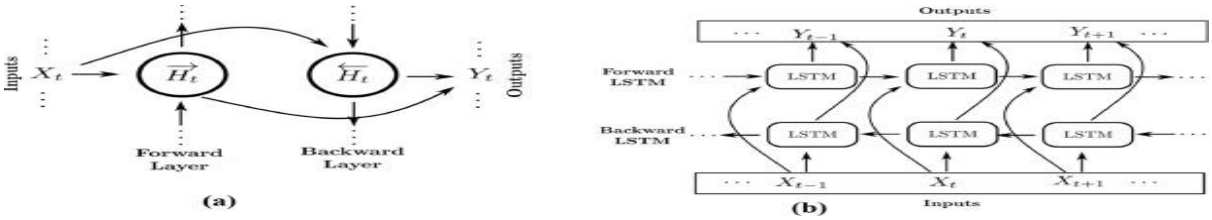

Figure 2.15. (a) Bidirectional RNN structure and (b) Bidirectional LSTM architecture schematic diagrams. (Graves & J. Schmidhuber ., 2005)

In instances when the context is necessary, the BiLSTM is beneficial. It has had widespread use in classification, most notably in text classification Z. Liu et al. (2020), sentiment classification A. Sharfuddin et al. (2018), and speech recognition A. Graves et al (2013) and load forecasting S. Wang et al. 2019.

2.7.3.4 GRU models

GRU was introduced as an alternative LSTM version by K. Cho et al. (2014), with the purpose of increasing LSTM performance, lowering the number of LSTM parameters, and simplifying its design. In GRU, the LSTM model's input and forget gates have been combined into a single gate known as an update gate. Instead of three gates, GRU has only two: update and reset gates. One of the novel features of GRUs models is the concept of reset and update gates. Following that, a novel evaluation method for computing hidden states in RNN models is presented. The GRU improves the LSTM structure by connecting the input and forget gates to the update gate and used the output gate as a reset gate.

2.7.3.5 Variational autoencoders

VAEs are generative models that use learned approximation inference and can be generated using gradient-based techniques. D.P. Kingma and colleagues (2013); D.J. Rezende and colleagues (2013) (2014). The phrase "in this context" is used "The statistical process known as "variational inference" is referred to as "variational." "The VAE is a regularized autoencoder that minimizes overfitting and produces a latent space with adequate qualities for the generating phase."" A simplified schematic illustration of the design of a VAE is shown in Figure 2.16. A VAE, like a traditional autoencoder, has both an encoder and a decoder. When training a VAE, the reconstruction error of the encoded-decoded data and the original input data is minimized. Using the latent space, the VAE converts the input data, X, into a distribution, q(z|x). See figure 2.16

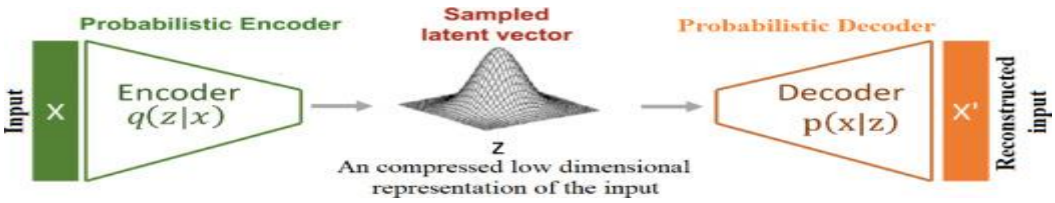

Figure 2.16. Schematic representation of Variational Autoencoders architecture (Rezende et al.,2013).

Because of its simplicity, versatility, and ease of implementation, the VAE framework has been extended to a variety of model architectures. For example, the deep recurrent attention writer is a more advanced version of VAE (DRAW). A recurrent encoder and decoder make up the attention mechanism in DRAW. VAE has been extended to construct sequences by introducing variational RNNs into the VAE system, which employs a recurrent encoder and decoder (J. Chung, et al., 2015; K. Gregor, et al., 2015).

CHAPTER 3: METHODOLOGY

3.1 Method

Models of convolutional neural networks Deep learning employs AlexNet and VGG. With a 3D CT scan as input, the system generates COVID-19 and normal class predictions. CT scanners are used to make 3D CT scans. A CT scan can provide clinicians with a three-dimensional image of the lungs of a patient. The axial, coronal, and sagittal planes are depicted in these 3D CT volumes. We use axial images (slices) from CT scans of patients in our method. An axial slice of a 3D CT scan is seen here. These cross-sections depict the human lungs from top to bottom. A three-category strategy is designed for arranging these axial slices. To diagnose Covid-19, we used artificial intelligence as well as deep learning methodologies such as Convolutional Neural Networks with models like AlexNet (fig 3.1) and VGG 16 (fig 3.3). On CT scan images from the Kaggle data set, the aforementioned methodologies are employed. Tables are created using data gathered from x-ray images, CT scans, and deep learning algorithms.

Convolutional Neural Networks (CNNs) were created to simulate the biological processes that occur in human vision. The networks used multiple layers and were arranged in a number of ways to form different networks or topologies. Traditional neural networks had three types of layers: fully connected layers, subsampling layers, and convolution layers.

Layers of Convolution

Convolution operations were performed using trainable kernels or filters in two-dimensional convolution layers, which occasionally included an optional trainable bias for each kernel. The kernels were moved over the input in strides throughout these convolution processes. The kernels skipped more spaces between each convolution as the stride increased. As a result, there were fewer overall convolutions but more microscopic ones. A multiplication operation was performed between the input section and the kernel for each placement of a specific kernel, with the bias added to the result. The outcome was a feature map that includes the convolved result. To give data for the following layer, feature maps were commonly delivered through an activation function. The feature map's size has been established.

Layers of Subsampling

Non-trainable kernels or windows were employed to down sample input characteristics in two-dimensional subsampling layers. This usually entailed a major reduction in the number of functions provided, as well as the network's reliance on location being removed. Average pooling and maximum pooling were the two most popular subsampling algorithms. Both methods employed the average or maximum of each kernel's values to build the final feature map. The size of the feature map for subsampling layers was estimated in the same way as the size of the feature map for convolution layers. To aid overall model learning, certain implementations of these layers contained trainable parameters.

Fully connected layers

Non-trainable kernels or windows were employed to down sample input characteristics in two-dimensional subsampling layers. This usually entailed a major reduction in the number of functions accessible and the elimination of a network's reliance on location. Average pooling and maximum pooling were the two most popular subsampling algorithms. Both methods employed the average or maximum of each kernel's values to build the final feature map. The size of the feature map for subsampling layers was estimated in the same way as the size of the feature map for convolution layers.In two-dimensional subsampling layers, non-trainable kernels or windows were used to down sample input characteristics. This usually entailed a major reduction in the number of functions accessible and the elimination of a network's reliance on location. Average pooling and maximum pooling were the two most popular subsampling algorithms. In all cases, the final feature map should include the average or maximum value of each kernel's values. The feature map size for subsampling layers was calculated in the same way as the feature map size for convolution layers was calculated.

3.1.1AlexNet Model

In image recognition, a CNN is used. In recent research, the CNN model is effective in extracting features, representing images, and retrieving images. The AlexNet model is used to extract picture feature information (Yuan & Zhang, 2016). AlexNet. Eight layers make up the architecture: There are five convolutional layers in total, as well as three completely linked layers. But that's not the only thing that sets AlexNet apart; here are some of the features that only convolutional neural networks have:

Nonlinearity. AlexNet employs Rectified Linear Units instead of the tanh function, which was popular at the time (ReLU). On the CIFAR-10 dataset, a CNN trained with ReLU was able to reach a 25% error six times faster than a CNN trained with tanh. Tanh or sigmoid non-linearity was the go-to activation function for modeling internal neuron activity within CNNs; this was the go-to activation function for training neurons within a neural network. After that, AlexNet used Rectified Linear Units, or ReLUs for short.

The ReLu operation is applied to the output of the preceding convolution layer. When ReLu is utilized, positive values within the neurons are maintained, while negative values are clamped to zero. ReLu allows the training process to be accelerated since gradient descent optimization happens at a faster rate than other non-linearity approaches. Network non-linearity is also introduced by the ReLu layer, which is a benefit. The associativity of subsequent convolutions, on the other hand, is lost.

Some graphics processing units (GPUs) are required. Previously, graphics processing units (GPUs) had 3 gigabytes of memory (nowadays those kinds of memory would be rookie numbers). The training set's 1.2 million photographs only made issues worse. By putting half of the model's neurons on one GPU and the other half on another, AlexNet enables for multi-GPU training. It enables for the training of larger models while simultaneously reducing training time. The original research paper that introduced the AlexNet neural network architecture used two GTX 580 GPUs with 3GB memory to train models.

Parallelization on the GPU and distributed training are two strategies that are widely used nowadays. The model was trained on two GPUs, with neurons of the model divided into two equal parts, according to the research article. The GPUs were able to communicate with one another without having to go via the host machine. Only specified layers can communicate with each other because communication between the GPU is restricted on a layer-by-layer basis. For example, half of the current GPU's third layer feature maps were used to construct the inputs in the AlexNet network's fourth layer, while the other half came from the second GPU.

Overlapping Pooling is a term used to describe a situation when two or more. The outputs of adjoining groups of neurons are generally "pooled" in CNNs. When the scientists added overlap, however, they detected a 0.5 percent drop in error and discovered that models with overlapping pooling are more difficult to overfit. In CNNs, pooling layers encapsulate

information within a set of pixels or values within a feature map and project it into a smaller grid while reflecting the general information from the original set of pixels. The diagram below is an example of pooling, specifically maximum pooling. Max pooling is a type of sub-sampling in which the maximum pixel value of pixels inside the pooling window's receptive field is used. A novel pooling mechanism was introduced and used in the work that describes the AlexNet CNN architecture.

3.1.1.1AlexNet Architecture

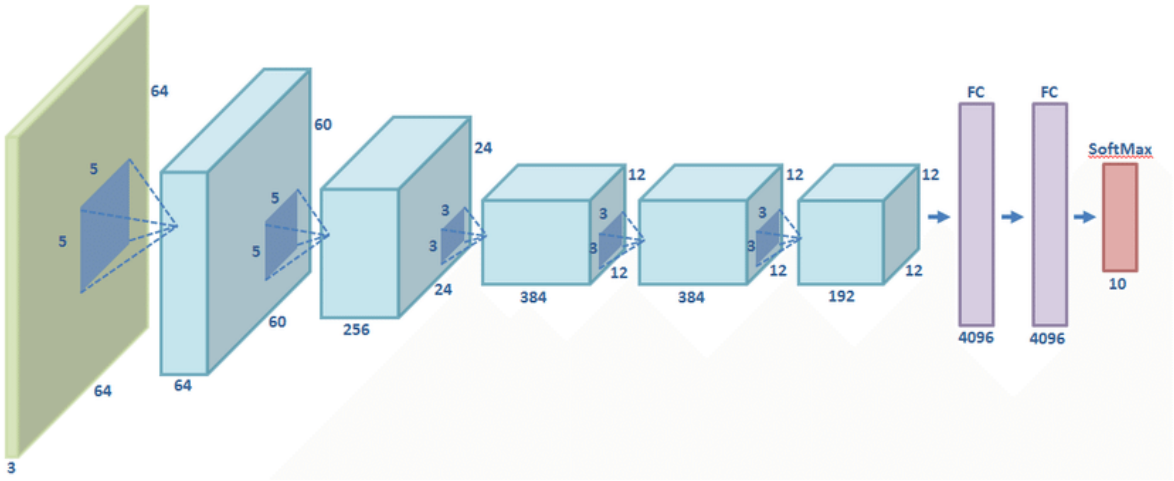

Figure3.1: The architecture of AlexNet. Krizhevsky et al. (2012) are responsible for the images.

AlexNet is credited with bringing deep learning to a variety of fields, including natural language processing and medical image analysis, as well as being a watershed moment in the spread of deep learning. It is a complex model capable of excellent accuracy on even the most challenging datasets. If a single layer is removed, its output will suffer greatly. AlexNet is a cutting-edge framework, with several applications in the artificial intelligence field of computer vision. AlexNet may be utilized for image tasks more than CNNs in the future. The Issue of Overfitting AlexNet contained 60 million parameters, which was a significant problem in terms of overfitting. To reduce overfitting, two strategies were used:

Augmentation of data. To make their data more diversified, the authors utilized label-preserving modification. They used horizontal reflections and photo translations to enlarge the training set by 2048 times. They also used Principal Component Analysis (PCA) on RGB pixel values to adjust the intensities of RGB channels, which resulted in a top-1 error rate of less than 1%.

Dropout. The "turning off" of neurons in this method requires a high degree of probability (e.g., 50 percent). Each cycle employs a distinct sample of the model's parameters, allowing each neuron to develop more resilient features that can be applied to subsequent neurons. Dropout, on the other hand, prolongs the model's convergence time.

Different layers in AlexNet(see figure 3.2)

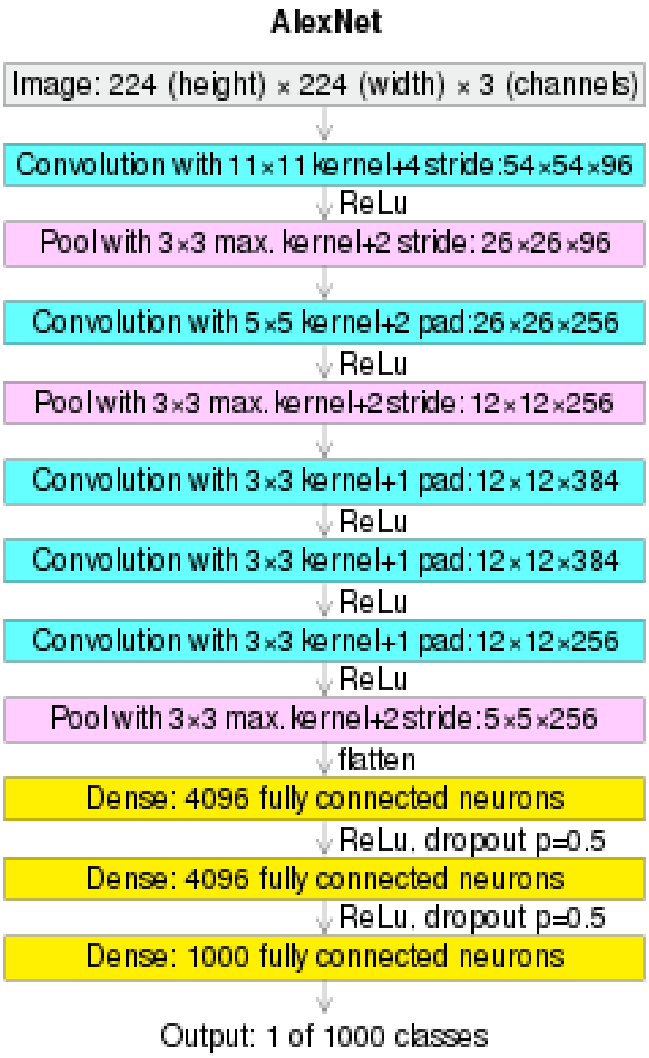

Figure 3.2: Different layers in AlexNet (Wei & Kehtarnavaz, 2018)

C1 has several layers: The first layer of convolution is: AlexNet's initial layer was a convolutional layer that took a (2242243) image tensor as input. It used 96 (1111) kernels with a 4 stride and two paddings in a convolution process. This produced a (555596) output tensor, which is then transmitted to the next layer using a ReLu activation function. The layer had 34,944 trainable parameters.

First Max Pooling Layer (S2): The second layer of AlexNet is a max-pooling layer that receives the result of layer C1 (555596) tensor as input. To do zero-padded subsampling, it used a (33) kernel with a stride of two. The output tensor was (272796), which was then passed on to the next layer.

C3: Second Convolution Layer: AlexNet's third layer was a convolutional layer that used the output of layer S2, which was a (272796) tensor, as input. It employed 256 kernels in a convolution process with a stride of one and padding of two. This technique produced a (2727256) output tensor, which was subsequently sent to the next layer after passing via a ReLu activation function. The layer had a total of 614,656 trainable parameters, bringing the total number of trainable parameters to 649,600.

S4: Second Max Pooling Layer: AlexNet's fourth layer was a max-pooling layer that took as input the result of layer C3, which was a (2727256) tensor. It uses a (33) kernel with a stride of two, similar to layer S2, to do zero-padded sub-sampling. This resulted in a (1313256) output tensor, which was then passed via a ReLU activation function before being passed on to the next layer.

C5: Third Convolution Layer: AlexNet's fifth layer was a convolutional layer that used the output of layer C5, which was a (1313256) tensor, as input. It utilized 384 (33) kernels with a stride and padding of one in a convolution process. The output tensor was (1313384), which was subsequently transmitted to the next layer using a ReLu activation function. The layer had 885,120 trainable parameters, making the total number of trainable parameters 1,534,720.

C6: Fourth Convolution Layer: The output of layer C5, a (1313384) tensor, was fed into AlexNet's sixth layer, which is a convolutional layer. It had a similar output size as layer C5 and used the same convolution approach. The output was also subjected to a ReLu activation function. The layer had 1,327,488 trainable parameters, totaling 2,862,208 trainable parameters.

C7: Fifth Convolution Layer: AlexNet's seventh layer is a convolutional layer that received a (1313384) tensor as input from layer C6. It used 256 (33) kernels in a convolution process with one stride and padding. The output tensor that resulted was (1313256). The output was also subjected to a ReLu activation function. The layer had a total of 3,747,200 trainable parameters, with 884,992 of those being trainable.

S8: Third Max Pooling Layer: The eighth layer of AlexNet is a max-pooling layer that got a (1313256) tensor from layer C7 as input. It created a zero-padded sub-sampling technique using a 33-window area with a stride of two, comparable to layers S2 and S4. This resulted in a (6628) output tensor, which was then passed through a ReLU activation function before moving on to the next layer.

F9: Fully Connected First Layer: AlexNet's ninth layer is a fully connected layer that received as input from layer S8 a flattened (66256) tensor. It made use of a weighted sum with a bias term. This resulted in a (40961) output tensor, which was then passed through a ReLu activation function before proceeding to the next layer. The layer contained 37,752,832 trainable parameters, for a total of 41,500,032.

F10: Second Fully Connected Layer: AlexNet's tenth layer is another fully linked layer that received a (40961) tensor from layer F9. It followed the same procedure as layer F9, resulting in the same (40961) output tensor, which is then processed through a ReLu activation function before proceeding to the next layer. The layer has 16,781,312 trainable parameters, bringing the total number of trainable parameters to 58,281,344 so far.

F11: Third Fully Connected Layer: The network's eleventh and final layer, Layer F10, is also a fully linked layer that received a (40961) tensor. It generated a (10001) output tensor, which was then routed via a softmax activation function, in the same way that layers F9 and F10 did. There are 4,097,000 trainable parameters in the layer, for a total of 62,378,344 trainable parameters. The network's predictions were included in the softmax activation function's output.

3.1.2 VGG model

Convolutional neural networks, or VGG models, are a type of convolutional neural network. VGG incorporates extra convolution layers and addresses a fundamental component of CNNs, unlike prior AlexNet derivatives, which concentrated on reduced frame widths and advancements in the first convolutional layer: depth. Let's take a closer look at VGG's architecture:

Input. VGG accepts RGB images with a resolution of 224x224 pixels as input. To keep the input picture size consistent for the ImageNet competition, the authors clipped out the middle 224x224 patch of each image.

The convolutional layers in this model have a limited receptive field (3x3, the smallest size that captures both left and right and up and down). Before the input is transferred to the ReLU unit, additional 1x1 convolution filters conduct a linear modification on it. The convolution stride is set at 1 pixel to retain spatial resolution after convolution.

The layers are all interconnected. VGG is made up of three entirely connected layers, each with 4096 channels, and the third with 1000 channels, one for each class.

Layers that are not visible with the naked eye. VGG's hidden layers all employ ReLU (a huge innovation from AlexNet that cut training time). Because it increases memory consumption and training time while delivering no benefit in accuracy, VGG does not use Local Response Normalization (LRN).

3.1.2.1 VGG configuration

The VGG network is divided into five configurations, labelled A through E. With more layers added, the configuration's depth rises from left (A) to right (B). The table below lists all of the possible network architectures. The table below shows the many VGG architectures. We can see that VGG-16 has two variants (C and D). There isn't much of a difference between them except for the fact that instead of using (3, 3) filter size convolution, they use (3, 3) and (1, 1) filter size convolution. There are 134 million and 138 million parameters in each of these. See table 3.1

Table 3.1: Different VGG Configuration

ConvNet Configuration					
A	A-LRN	B	C	D	E
11 weight layers	11 weight layers	13 weight layers	16 weight layers	16 weight layers	19 weight layers
input (224 × 224 RGB image)					
conv3-64	conv3-64 **LRN**	conv3-64 **conv3-64**	conv3-64 conv3-64	conv3-64 conv3-64	conv3-64 conv3-64
maxpool					
conv3-128	conv3-128	conv3-128 **conv3-128**	conv3-128 conv3-128	conv3-128 conv3-128	conv3-128 conv3-128
maxpool					
conv3-256 conv3-256	conv3-256 conv3-256	conv3-256 conv3-256	conv3-256 conv3-256 **conv1-256**	conv3-256 conv3-256 **conv3-256**	conv3-256 conv3-256 conv3-256 **conv3-256**
maxpool					
conv3-512 conv3-512	conv3-512 conv3-512	conv3-512 conv3-512	conv3-512 conv3-512 **conv1-512**	conv3-512 conv3-512 **conv3-512**	conv3-512 conv3-512 conv3-512 **conv3-512**
maxpool					
conv3-512 conv3-512	conv3-512 conv3-512	conv3-512 conv3-512	conv3-512 conv3-512 **conv1-512**	conv3-512 conv3-512 **conv3-512**	conv3-512 conv3-512 conv3-512 **conv3-512**
maxpool					
FC-4096					
FC-4096					
FC-1000					
soft-max					

3.1.2.2 VGG Architecture (VGG 16)

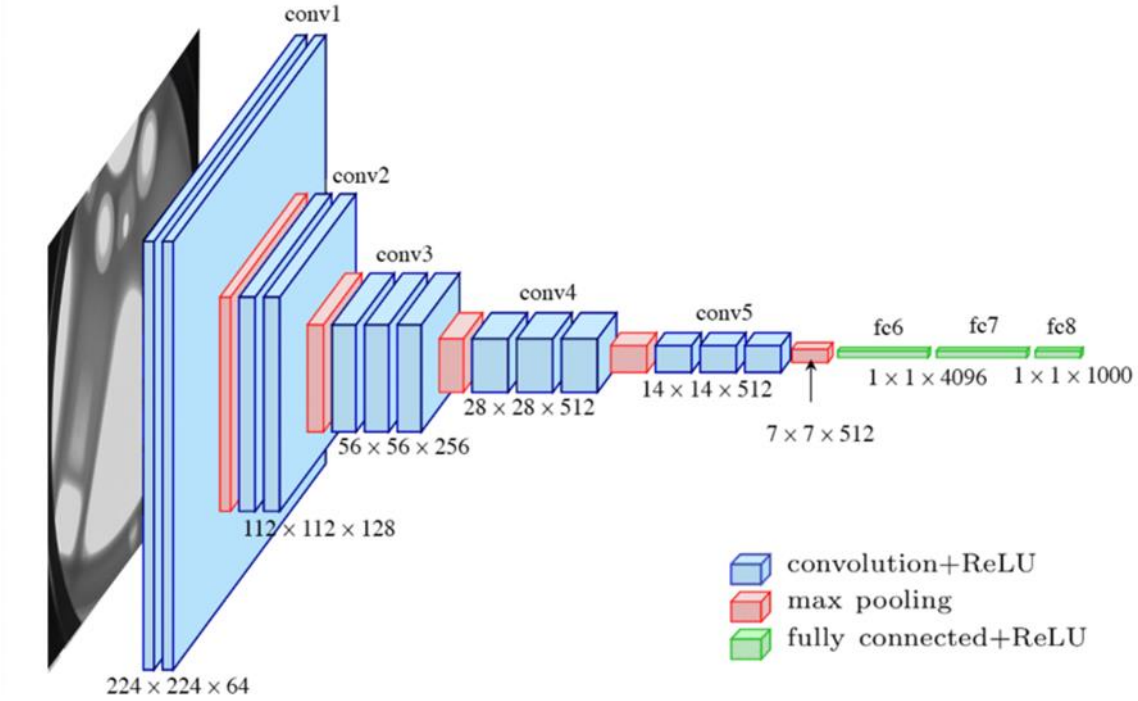

Figure 3.3: Simonyan K. and Zisserman A.'s suggested standard VGG-16 network design (2016) The feature extractor only uses layers "conv1" through "fc7."

The input to the cov1 layer is a 224 224 RGB picture with a fixed size. A convolutional (Conv.) layer stack with a very narrow receptive field of 33 (the minimum size to capture the notions of left/right, up/down, and center) is utilized to process the image. It also uses 11 convolution filters in one of the settings, which can be thought of as a linear change of the input channels (followed by non-linearity).

All buried layers have the rectification non-linearity (ReLU). Except for one, none of the networks apply Local Response Normalization (LRN), which uses more memory and takes longer to compute while boosting performance on the ILSVRC dataset. There are 16 model layers in VGG. See figure 3.4

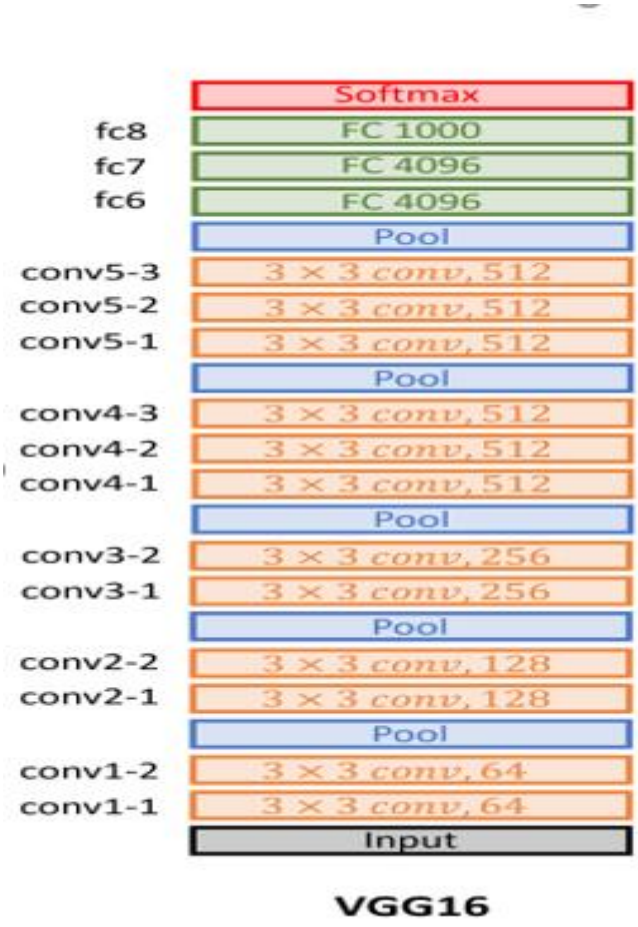

Figure 3.4 : layers of VGG 16 model(Tammina,2019)

The first two layers are convolutional layers with 3x3 filters, according to fig. 3.4, and the first two layers use 64 filters, resulting in a volume of 224x224x64 due to the use of the same convolutions. The filters are always 3x3 with a single stride. The volume's height and width were reduced from 224x224x64 to 112x112x64 using a pooling layer with a max-

pool of 2x2 size and stride 2. There are two more convolution layers after that, each with 128 filters. The new dimension is 112x112x128 as a result. After applying the pooling layer, the volume is reduced to 56x56x128. Two further 256-filter convolution layers are added, each followed by a down sampling layer, bringing the total size down to 28x28x256. Two further stacks, each with three convolution layers, are separated by a max-pool layer. After the final pooling layer, the 7x7x512 volume is flattened into a Fully Connected (FC) layer with 4096 channels and a softmax output of 1000 classes.

VGG16 has sixteen layers of varying weights, hence the name. This fairly large network is made up of 138 million parameters. Even by today's standards, that's a substantial sum of money. The VGG16 design, on the other hand, piqued my interest because of its simplicity. This architecture has a lot of consistency. To reduce the volume's height and breadth, an extra pooling layer is utilised. Looking at the number of filters utilised, we can see that we start with 64 filters, then go on to 128 and 256, and eventually 512 filters.Every step or stack of convolutional layers doubles the number of filters used, and this is another fundamental concept used to design the architecture of this network. As a result, there were a plethora of factors to teach, which was a drawback. However, because VGG16 performs almost as well as VGG19, we will go with VGG16.

3.1.3 Comparison between AlexNet and VGG Net

AlexNet is the first large-scale convolutional neural network to use ImageNet to identify images. AlexNet surpassed all prior non-deep learning-based models in the competition.

A convolution layer, a pooling layer, normalization, Conv-pool-norm, a few more convolution layers, a pooling layer, and a plethora of fully linked layers make up AlexNet's architecture. It's similar to the LeNet system. Simply put, there are more levels in total. Before the last linked layer that leads to the output classes, there are five Conv layers and two completely connected layers.

On ImageNet, AlexNet was trained with 227x227 x 3 picture inputs. AlexNet's conv layer has 11x11 filters, with 96 of them being utilised at stride 4. The final image included 35K parameters in the first layer and measured 55 x 55 x 96 pixels. At stride 2, we have three 3 x 3 filters applied to the second layer, which is a pooling layer. The pooling layer's output volume with a 0 parameter to learn is 27 x 27 x 96. Because the parameters are the weights attempting to learn, the pooling layer learns nothing.

The 11 by 11 filters come first, followed by 5 by 5 filters and a few three-by-three filters.Finally, there are two 4096-layer fully linked layers, with FC8 connecting to the softmax, which connects to 1000 ImageNet classes. The ReLu non-linearity is used in this design for the first time.

For the first time, the ReLU non-linearity is applied in this design. AlexNet also makes use of a normalizing layer. Data enhancement techniques such as flipping, jittering, cropping, colornormalization, and others were used by AlexNet. Dropout is 0.5, SGD + Momentum is 0.9, and the initial learning rate is 1e-2, a factor of ten lower when the validation accuracy is flat. This network's regularization is L2, with a weight decay of 5e-4. It has a GTX580 graphics card and 3GB of RAM. The ImageNet Large Scale Visual Recognition Challenge has a mistake rate of 16.4 percent (ILSVRC).

In 2014, a few designs were noticeably different and achieved yet another performance boost, with their size being the point of separation between them.

There are 16 layers in the VGG 16 design, including two convolution layers, a pooling layer, and a fully linked layer at the bottom. Larger networks with smaller filters are the foundation of the VGG network. VGG Net has more layers than AlexNet, which only has eight. At the time, VGG Net models with 16 to 19 layers were available. These models all employed 3 x 3 conv filters, the smallest conv filter size that only looks at a small percentage of the nearby pixels. And they effectively maintained a 3 x 3 conv architecture with some network pooling on occasion.

VGG used tiny filters and stacked them instead of larger filters because there were fewer parameters. Instead of large filters, VGG employs smaller, deeper filters. The effective receptive field is now the same as if there were only one 7 x 7 convolutional layer.

Many convolutional layers, a pooling layer, several more convolutional layers, a pooling layer, and so on are included in VGG Net. The VGG architecture consists of 16 convolutional and fully connected layers in total. For VGG 16, it has 16 layers. It's designed in the same way as the previous one, but with a few more conv levels.

So, with 138 million total parameters and each image having a memory of 96 megabytes, this is a very expensive computation. The ILSVRC challenge has a 7.3 mistake rate.

3.2 Data set description

The development of AI-powered COVID-19 diagnostic tools based on CTs is hampered by the difficulty of obtaining publicly available COVID-19 CT datasets due to privacy issues. To solve this problem, we sought for existing COVID-CT datasets and settled on the Kaggle Covid-19 CT scan dataset, which has 205 COVID-19 and non-COVID-19 CT images. The dataset's utility has been validated by a well-known radiologist who has been treating and diagnosing COVID-19 patients since the outbreak began. Further research suggests that this dataset could be used to develop AI-based COVID-19 diagnostic algorithms.

CHAPTER 4: RESULTS AND FUTURE WORKS

4.1 Results

This section presents model performance findings based on their ability to detect even trace amounts of covid-19 in chest CT images. We considered Kaggle dataset and used 205 images that are classified under a different type of pneumonia. There was a lot of improvement and benefits of utilizing these convolutional neural networks (CNN) models after model training and assessment with Alex Net and VGG. 60% of the images were used to train the model, while forty percent are used for testing. The models' performance is evaluated using testing accuracy, sensitivity, and specificity. To acquire preliminary results, 205 CT scans of COVID-19 and non-COVID-19, bacterial pneumonia, and healthy pictures were employed. Due to the insufficient amount of data, we have low accuracy, sensitivity, and specificity. Because we only have 205 COVID-19 CT scans, we did this study to test the dataset's linearity by using the same number of training and testing datasets. The Kaggle dataset is used to assess the performance of the suggested deep learning approach. The metrics listed below are used to assess performance. The accuracy of the approaches is assessed using the performance metrics area under the receiver operating characteristic (ROC) curve (AUC), accuracy (ACC), sensitivity (SE), and specificity (SP). The following are the definitions of accuracy, sensitivity, and specificity:

Accuracy = $\frac{TP+TN}{TP+TN+FN+FP}$ ……………………… (1)

Sensitivity = $\frac{TP}{TP+FN}$ ……………………………. (2)

Specificity = $\frac{TN}{TN+FP}$ …………………………......(3)

where TP, TN, FP, and FN indicate true positive, true negative, false positive, and false negative, respectively.

After using the above parameters, the results obtained from both models is illustrated in the table below. See table 4.1

Table 4.1: Summary of performance evaluation parameters

Network	Disease	Data	AUC	ACC	SE	SP
Alex Net	COVID-CT	Aug	0.60	0.67	0.72	0.64
VGG	COVID-CT	Aug	0.65	0.75	0.86	0.70

From table 6, we can see the different results obtained from our method.

ROC curve that evaluates a classifier's ability to differentiate between classes and it is described by the matrix AUC. With rising AUC, the model's ability to distinguish between positive and negative classes increases; we have 0.60 and 0.65 for AlexNet and VGG, respectively. The AUC is higher than normal, indicating that the models are suitable for usage.

Measures such as how often a machine learning classification algorithm identifies a data point properly are known as the accuracy of the algorithm. Accuracy is the percentage ofdata points properly predicted among all the data points and in our method, we had 0.67 and 0.75 for AlexNet and VGG respectively.

The model can predict real positive results in each category that's measured by sensitivity. To determine a model's specificity, look at how well it can predict true negatives in each of the given categories. Our models prove to be highly sensitive 0.72 and 0.86 for AlexNet and VGG respectively.

Specificity is the percentage of negatives that were anticipated as true negatives. This means that there will be a further fraction of real negatives which were projected as positive and maybe called false positives. It's possible to refer to this percentage as the false-positive rate, the models are indeed effective with a specificity of 0.64 and 0.70 for AlexNet and VGG respectively.

Comparison between the results obtained using AlexNet and VGG models

Table 6 gives a summary of the results from the two models AlexNet and VGG used in this study. They both gave good results but we noticed that for any of the parameters, but VGG is better than AlexNet with greater values in all the parameters which could be as a result of more convolution layers.

4.2 Future Works

How many of these applications will be clinically useful is unknown. The first step toward this goal is to identify the clinical need for which a solution could improve or change clinical treatment. Applied AI research is impossible to do without appropriate clinical oversight, thus risks producing solutions then search for problems: a type of supply seeking demand rather than demand seeking supply. Despite the widespread publication of AI-

based diagnostic medical research, the number of systems that have been validated in clinical trials and implemented in clinical practice remains limited. The COVID-19 research objectives, on the other hand, risk being overly focused on developing novel deep learning models without thoroughly analyzing their practical utility and biases. Deep learning algorithm speed and accuracy are sometimes stated based on clinical scenarios that may not be completely representative of real-world practice. Comparisons of computer vs. human performance may be inconsistent at times. A computer is typically configured to detect a specific anomaly (such as COVID-19-related illness), whereas a radiologist is in charge of identifying any abnormality (including incidental findings such as pulmonary nodules). Deep learning-based CT analysis beat viral real-time PCR testing as a valid COVID-19 screening approach in at least one investigation. However, these findings should be interpreted with caution. Because of the artificially high illness prevalence and the type of people chosen, whose illness severity necessitated hospitalization and CT scans, pandemic research was inherently dangerous.

CHAPTER 5: CONCLUSION AND DISCUSSION

SARS-CoV-2, a novel COVID-19-causing coronavirus, has wreaked havoc on global healthcare systems. In some countries, demand for personal protection equipment and ventilators has outstripped supply, resulting in an unusual demand for the latter due to the risk of respiratory syndrome that comes with such illness. Concerning covid-19, there are two imaging diagnostic modalities that are chest x-ray and CT scan commonly used and these two have generated massive amounts of data used in building algorithms in AI precisely deep learning algorithms. Deep learning-based technologies in medical imaging have gained a lot of traction even before the COVID-19 outbreak. Massive datasets from China, and more often from countries in Europe, have resulted in a spate of COVID-19 articles describing AI applications. COVID-19 patients are growing at an exponential rate, placing strain on healthcare systems worldwide. It is impossible to screen every patient with a respiratory illness using standard procedures due to the restricted number of testing kits available (RT-PCR). Furthermore, the tests are time-consuming and have limited sensitivity, necessitating the use of experienced experts and a radiologist. VGG and Alex Net, the two deep learning models we employed, exhibited substantial improvement in the identification and prediction of covid 19. In publicly available covid-chest CT scan dataset, our model predicts COVID-19 infection with greater than 75% accuracy and 85% sensitivity.

REFERENCE

Ahmad J., Farman H., Jan Z. (2019) Deep Learning Methods and Applications. In: Deep Learning: Convergence to Big Data Analytics. Springer Briefs in Computer Science. Springer, Singapore.

Angelov, P., & Soares, E. (2020). EXPLAINABLE-BY-DESIGN APPROACH FOR COVID-19 CLASSIFICATION VIA CT-SCAN. DOI: 10.1101/2020.04.24.20078584

AshourA.S., El-AttarA., DeyN., El-KaderH.A, El-NabyM.A (2020). Long short-term memory-based patient-dependent model for FOG detection in Parkinson's disease. Pattern Recognit Lett, 131 (2020), pp. 23-29

Asif Iqbal Khan, Junaid Latief Shah, Mohammad Mudasir Bhat, (2020). CoroNet: A deep neural network for detection and diagnosis of COVID-19 from chest x-ray images, Computer Methods and Programs in Biomedicine, Volume 196, 2020, Article 105581

Bernheim A, Mei X, Huang M, Yang Y, Fayad ZA, Zhang N., (2020). Chest CT Findings in Coronavirus Disease-19 (COVID-19): Relationship to Duration of Infection. Radiology. 2020:200463

Bjorke, H. Covid-19 segmentation dataset. MedSeg http://medicalsegmentation.com/covid19/ (2020).

Chest X-ray images (pneumonia). https://www.kaggle.com/ paultimothymooney/chest-xray-pneumonia. Last Accessed: 1 Apr 2020.

Chartrand, G., Cheng, P.M., Vorontsov, E., 2017. Deep learning: a primer for radiologists. Radiographics 37, 2113–2131

ChoK., Van MerriënboerB., GulcehreC., BahdanauD., BougaresF., SchwenkH. (2014). Learning phrase representations using RNN encoder-decoder for statistical machine translation (2014), arXiv:14061078

Cohen, J. P., Morrison, P. & Dao, L. (2020). Covid-19 image data collection. Preprint at http://arxiv.org/abs/2003.11597 (2020).

Dhawan, A. P. (2011). Medical Imaging Modalities: X-Ray Imaging. Medical Image Analysis 79–97, https://doi.org/10.1002/9780470918548.ch4 (2011).

Erickson, B.J., Korfiatis, P., Akkus, Z.,2017. Machine learning for medical imaging. Radiographics 37, 505–515.

GravesA., JaitlyN., MohamedA. (2013). Hybrid speech recognition with deep bidirectional LSTM, 2013 IEEE workshop on automatic speech recognition and understanding, IEEE (2013), pp. 273-278

Graves A., Schmidhuber J. (2005). Framewise phoneme classification with bidirectional LSTM and other neural network architectures. Neural Netw, 18 (5–6) (2005), pp. 602-610

Gregor K., DanihelkaI.,GravesA., RezendeD.J., WierstraD. (2015). Draw: a recurrent neural network for image generation (2015)

Harmon, S., Sanford, T., Xu, S., Turkbey, E., Roth, H., & Xu, Z. et al. (2020). Artificial intelligence for the detection of COVID-19 pneumonia on chest CT using multinational datasets. Nature Communications, 11(1). doi: 10.1038/s41467-020-17971-2

Hinton G et al (2012) Deep neural networks for acoustic modelling in speech recognition: the shared views of four research groups. IEEE Signal Process Mag 29:82–97

Hochreiter S., J. Schmidhuber J. (1997). Long short-term memory.NeuralComput, 9 (8) (1997), pp. 1735-1780

Harrou F., Kadri F., Sun Y. (2020). Forecasting of photovoltaic solar power production using the LSTM approach. Advanced statistical modelling, forecasting, and fault detection in renewable energy systems, Intech Open (2020)

Huang C, Wang Y, Li X, Ren L, Zhao J, Hu Y., (2020). Clinical features of patients infected with 2019 novel coronavirus in Wuhan, China. Lancet. 2020;395(10223):497–506.

Irvin J., Rajpurkar P., Ko M., Yu Y., Ciurea-Ilcus S., Chute C., Marklund H., Haghgoo B, Ball R, Shpanskaya, K (2019). Chexpert: a large chest radiograph dataset with uncertainty labels and expert comparison, Proc. AAAI Conf. Artif. Intell. (2019), pp. 590-597

Ismael, A., Şengür, A. (2021). Deep learning approaches for COVID-19 detection based on chest X-ray images. Expert Systems with Applications, 164, 114054.

J. Chung, K. Kastner, L. Dinh, K. Goel, A.C. Courville, Y. Bengio (2015). A recurrent latent variable model for sequential data. Advances in neural information processing systems (2015), pp. 2980-2988

Jacob, J., Alexander, D., Baillie, J., Berka, R., Bertolli, O., & Blackwood, J. et al. (2020). Using imaging to combat a pandemic: rationale for developing the UK National COVID-19Chest Imaging Database. European Respiratory Journal, 56(2), 2001809. DOI: 10.1183/13993003.01809-2020

Jiang Na, Yang Haiyan, Gu Qingchuan, Huang Jiya. Machine learning and its algorithm and development analysis [J]. Information and Computer Science (Theoretical Edition), 2019 (01): 83-84 + 87.

Jun, M. (2020). Covid-19 ct lung and infection segmentation dataset (version version 1.0). Zenodo https://doi.org/10.5281/zenodo.3757476 (2020).

Junyoung Chung, Kyle Kastner, Laurent Dinh, Kratarth Goel, Aaron Courville, Yoshua Bengio. (2016). A Recurrent Latent Variable Model for Sequential Data

Katsevich, A. (2002). Theoretically Exact Filtered BackProjection-Type Inversion Algorithm for Spiral CT. SIAM Journal on Applied Mathematics 62, 2012–2026, https://doi.org/10.1137/S0036139901387186 (2002)

Kingma,D.P. (2013). Fast gradient-based inference with continuous latent variable models in auxiliary form (2013), arXiv preprint arXiv:13060733.

Khan, A., Shah, J., & Bhat, M. (2020). CoroNet: A deep neural network for detection and diagnosis of COVID-19 from chest x-ray images. Computer Methods and Programs in Biomedicine, 196, 105581.

Kushwaha, S., Bahl, S., Bagha, A. K., Parmar, K. S., Javaid, M., Haleem, A., & Singh, R. P. (2020). Significant applications of machine learning for a covid-19 pandemic. Journal of Industrial Integration and Management, 5(4).

Kwee, T., & Kwee, R. (2020). Chest CT in COVID-19: What the Radiologist Needs to Know. Radiographics, 40(7), 1848-1865.

Lassau, N., Ammari, S., Chouzenoux, E., Gortais, H., Herent, P., &Devilder, M. et al. (2021). Integrating deep learning CT-scan model, biological and clinical variables to predict severity of COVID-19 patients. Nature Communications, 12(1). doi: 10.1038/s41467-020-20657-4.

Le Cun Y, Bengio Y, Hinton G (2015) Deep learning. Nature 521:436–444

Li Kanghua, Jiang Shan. Machine Learning and Cultural Production Reform-Based on the Perspective of the Development of AI Technology [J]. Journal of Xiangtan University (Philosophy and Social Sciences), 2020, 44 (01): 74-79.

Li, X., Geng, M., Peng, Y., Meng, L., & Lu, S. (2020). Molecular immune pathogenesis and diagnosis of COVID-19. Journal of Pharmaceutical Analysis, 10(2), 102-108.

Li Y, Xia L., (2020). Coronavirus Disease 2019 (COVID-19): Role of Chest CT in Diagnosis and Management. AJR Am J Roentgenol. 2020:1–7.

Liu Z.-x., Zhang D.-g, Luo G.-z., Lian M., Liu B. (2020). A new method of emotional analysis based on CNN–BiLSTM hybrid neural network, Cluster Comput (2020), pp. 1-13.

Maguolo, G., & Nanni, L. (2021). A critic evaluation of methods for COVID-19 automatic detection from X-ray images. Information Fusion, 76, 1-7. https://doi.org/10.1016/j.inffus.2021.04.008

Morozov, S. et al. (2020). Mosmeddata: Chest ct scans with covid-19 related findings dataset. Preprint at https://arxiv.org/abs/2005.06465 (2020).

Naudé, Wim, Artificial Intelligence Against Covid-19: An Early Review. IZA Discussion Paper No. 13110, Available at SSRN: https://ssrn.com/abstract=3568314

Ozsahin, I., Sekeroglu, B., Musa, M., Mustapha, M., & Uzun Ozsahin, D. (2020). Review on Diagnosis of COVID-19 from Chest CT Images Using Artificial Intelligence. Computational And Mathematical Methods In Medicine, 2020, 1-10. doi: 10.1155/2020/9756518

Panwar, H., Gupta, P., Siddiqui, M., Morales-Menendez, R., Bhardwaj, P., & Singh, V. (2020). A deep learning and grad-CAM based color visualization approach for fast detection of

COVID-19 cases using chest X-ray and CT-Scan images. Chaos, Solitons & Fractals, 140, 110190. doi: 10.1016/j.chaos.2020.110190

Radiology Assistant. (2020). X-ray Chest images [dataset]. Retrieved March 23, 2020, from https://radiologyassistant.nl/chest/lk-jg-1

Rahimzadeh, M., Attar, A., &Sakhaei, S. (2021). A fully automated deep learning-based network for detecting COVID-19 from a new and large lung CT scan dataset. Biomedical Signal Processing And Control, 68, 102588. DOI: 10.1016/j.bspc.2021.102588

RezendeD.J, MohamedS., WierstraD. (2014). Stochastic backpropagation and approximate inference in deep generative models (2014), arXiv preprint arXiv:14014082.

Rubin GD, Haramati LB, Kanne JP, Schluger NW, Yim JJ, Anderson DJ, (2020). The Role of Chest Imaging in Patient Management during the COVID-19 Pandemic: A Multinational Consensus Statement from the Fleischner Society. Radiology. 2020:201365.

Schuster M., Paliwal K.K. (1997). Bidirectional recurrent neural networks. IEEE Trans Signal Process, 45 (11) (1997), pp. 2673-2681

Shah, V., Keniya, R., Shridharani, A., Punjabi, M., Shah, J., & Mehendale, N. (2021). Diagnosis of COVID-19 using CT scan images and deep learning techniques. Emergency Radiology.

Sharfuddin A.A., Tihami M.N., Islam M.S. (2018). A deep recurrent neural network with BiLSTM model for sentiment classification 2018 International conference on Bangla speech and language processing (ICBSLP), IEEE (2018), pp. 1-4

Simonyan K. & Zisserman A. (2014) “Very deep convolutional networks for large-scale image recognition,” arXiv preprint arXiv:1409.1556.

WangS., WangX., WangS., WangD. (2019). Bi-directional long short-term memory method based on attention mechanism and rolling update for short-term load forecasting, Int J Electr Power Energy Syst, 109 (2019), pp. 470-479

Wang X., Peng Y., Lu L., Lu Z., Bagheri M., Summers R.M. (2017). Chestx-ray8: hospital-scale chest x-ray database and benchmarks on weakly-supervised classification and localization of common thorax diseases Proc. IEEE Conf. Comput. Vis. Pattern Recognit (2017), pp. 2097-2106.

World Health Organization. WHO announces COVID-19 outbreak a pandemic. http://www.euro.who.int/en/health-topics/health-emergencies/coronavirus-covid-19/news/news/2020/3/who-announces-covid-19-outbreak-a-pandemic. Published March 12, 2020. Accessed June 6, 2020

Xie X, Zhong Z, Zhao W, Zheng C, Wang F, Liu J., (2020). Chest CT for Typical 2019-nCoV Pneumonia: Relationship to Negative RT-PCR Testing. Radiology. 2020:200343

Yuki, K., Fujiogi, M., &Koutsogiannaki, S. (2020). COVID-19 pathophysiology: A review. Clinical Immunology, 215, 108427.

Zeroual, A., Harrou, F., Dairi, A., & Sun, Y. (2020). Deep learning methods for forecasting COVID-19 time-Series data: A Comparative Study. Chaos, Solitons & Fractals, 140, 110121.

ZhangB., ZhangH., ZhaoG., LianJ., (2020). Constructing a PM2.5 concentration prediction model by combining auto-encoder with Bi-LSTM neural networks, Environ Modell Softwear, 124 (2020), p. 104600

Zhai, P., Ding, Y., Wu, X., Long, J., Zhong, Y., & Li, Y. (2020). The epidemiology, diagnosis and treatment of COVID-19. International Journal of Antimicrobial Agents, 55(5), 105955.

Zhao, J., Zhang, Y., He, X. & Xie, P. 92020). Covid-CT-dataset: a CT scan dataset about covid-19. Preprint at https://arxiv.org/abs/2003.13865 (2020).

Z. Yuan and J. Zhang (2016). AlexNet-based feature extraction and picture retrieval. The Eighth International Conference on Digital Image Processing is a gathering of experts in the field of digital image processing (ICDIP 2016). https://doi.org/10.1117/12.2243849

APPENDICES

Appendix 1: Ethical Approval Document

ETHICAL APPROVAL DOCUMENT

DATE:

To the Institute of Graduate Studies,

For the thesis project entitled as “ARTIFICIAL INTELLIGENCE APPLICATION IN COVID-19 DIAGNOSIS AND PREDICTION USING BY CT SCAN” the researchers declare that they did not collect data from human, animal or any other subjects. Therefore, this project does not need to go through the ethics committee evaluation.

Title: Assoc. Prof. Dr

Name surname: SERTAN SERTE

Signature:

Role in the Research Project: Supervisor